catalysts

MDPI

Review

Research Progress on Metal Oxides for the Selective Catalytic Reduction of NO_x with Ammonia

Lanyi Wang [1], Shengran Zhou [1], Mengxia You [2], Di Yu [2], Chunlei Zhang [1], Siyu Gao [1], Xuehua Yu [1,*] and Zhen Zhao [1,2,*]

[1] Institute of Catalysis for Energy and Environment, College of Chemistry and Chemical Engineering, Shenyang Normal University, Shenyang 110034, China; wanglanyii@163.com (L.W.); zhoushengran1997@163.com (S.Z.); zhangchunlei0423@163.com (C.Z.); gsy990328@163.com (S.G.)

[2] State Key Laboratory of Heavy Oil Processing, China University of Petroleum, 18# Fuxue Road, Beijing 102249, China; youmengxia258@163.com (M.Y.); yudii1127@163.com (D.Y.)

* Correspondence: yuxuehua1986@163.com (X.Y.); zhenzhao@cup.edu.cn or zhaozhen1586@163.com (Z.Z.)

Abstract: Nitrogen oxides emitted from diesel vehicle exhaust seriously endanger the atmospheric environment and human health, which have attracted people's attention. Among numerous nitrogen oxide (NO_x) removal technologies, photocatalytic removal of NO_x and SCR have received widespread attention. The photocatalytic treatment of NO_x technology is a good choice due to its mild reaction conditions and low costs. Moreover, NH_3-SCR has been widely used in denitration technology and plays an important role in controlling NO_x emissions. In NH_3-SCR technology, the development of high-efficiency catalysts is an important part. This paper summarizes the research progress of metal oxide catalysts for NH_3-SCR reactions, including V-based catalysts, Mn-based catalysts, Fe-based catalysts, Ce-based catalysts, and Cu-based catalysts. Meanwhile, the detailed process of the NH_3-SCR reaction was also introduced. In addition, this paper also describes a possible SO_2 poisoning mechanism and the stability of the catalysts. Finally, the problems and prospects of metal oxide catalysts for NO_x removal were also proposed.

Keywords: metal oxides; NH_3-SCR; catalytic performance; SO_2 and H_2O poisoning

check for updates

Citation: Wang, L.; Zhou, S.; You, M.; Yu, D.; Zhang, C.; Gao, S.; Yu, X.; Zhao, Z. Research Progress on Metal Oxides for the Selective Catalytic Reduction of NO_x with Ammonia. *Catalysts* **2023**, *13*, 1086. https://doi.org/10.3390/catal13071086

Academic Editor: Eleni Iliopoulou

Received: 30 May 2023
Revised: 1 July 2023
Accepted: 5 July 2023
Published: 11 July 2023

1. Introduction

With an increase in the number of vehicles globally, there has been an increase in pollution from vehicle exhaust [1]. Of the gases present in vehicle exhaust, nitrogen oxides (NO_x) are one of the most serious pollutants, causing air pollution that leads to acid rain, ozone depletion, and the greenhouse effect [2,3]. Moreover, NO_x also poses a huge threat to human health as it damages the human body through contact, inhalation, etc. [4]. Moreover, it has been reported that people with asthma may experience chronic pulmonary dilation and exacerbation of respiratory symptoms within 60 min of being exposed to nitrogen dioxide (NO_2) [5]. As NO_x gases pose such a serious threat to the human body and environment, the removal of NO_x is essential. Removal technologies for NO_x mainly include selective catalytic reduction (SCR), selective non-catalytic reduction (SNCR), activated carbon adsorption methods, photocatalytic degradation, and advanced oxidation processes (AOPs) based on ozone oxidation [6]. Generally, SCR technology involves reacting NO with reducing agents, such as gaseous ammonia (NH_3), liquid NH_3, and urea in the presence of a catalyst, whereas SNCR involves injecting a reducing agent into a system in a suitable "temperature window" to promote a denitration reaction without a catalyst to reduce NO_x to nitrogen and water. Activated carbon has a high adsorption capacity for a low concentration of NO_x. However, due to the possibility of spontaneous combustion of the activated carbon at >300 °C, its use poses significant difficulties for adsorption and regeneration. Photocatalytic degradation is a pollutant control technology that has the advantages of mild reaction conditions and producing a low amount of secondary pollution [7]. The

photocatalytic reactor is the core equipment in photocatalytic technology and its efficiency is influenced by many factors, such as light source, catalyst properties, and temperature. Therefore, designing a perfect reactor is crucial for enhancing NO_x removal efficiency. This also indicates that the design of reactors plays a very important role in photocatalytic technology. Moreover, the catalytic removal of NO_x using the semiconductor TiO_2 as a photocatalyst is very effective. Khanal et al. [8] prepared ultrafine Ta_2O_5 nanoparticles and tested the photodegradation of NO_x under UV–vis irradiation at room temperature. Compared with commercially available TiO_2, which is traditionally considered to be the most advanced NO_x degradation material, the ultrafine Ta_2O_5 nanoparticles exhibited a higher NO conversion. AOPs based on ozone oxidation for denitration mainly utilize ozone to oxidize NO_x, which is then absorbed by a washing tower for removal. This denitration system efficiently removes pollutants such as NO_x, sulfur dioxide, and particulate matter simultaneously, without affecting other pollutant control technologies. Thus, it is an efficient supplementary or alternative technology to traditional denitration technology. Alumina, as a representative ozone catalyst, is highly efficient, has a long lifespan, is cheap, and can remove more harmful gases from the exhaust in a shorter time than other catalysts. Table 1 summarizes the methods of NO_x removal mentioned above, as well as their catalysts and performance.

Table 1. The NO_x removal technologies as well as representative catalysts and performance.

Removal Technologies of NO_x	Representative Catalysts and Their Performance
SCR	V_2O_3-WO_3/TiO_2 catalysts exhibit the satisfactory catalytic performance in the medium temperature range
SNCR	-
Activated carbon adsorption	Activated carbon adsorbs low concentration NO_x at temperatures below 300 °C
Photocatalytic degradation	Commercially available TiO_2 has the excellent NO removal effect
Advanced oxidation processes (AOPs) ozone oxidation	Al_2O_3 catalyst has the higher oxidation efficiency and longer lifespan

Currently, hybrid systems involving the simultaneous use of multiple techniques are also a hot research topic, such as technology for the simultaneous removal of soot and NO_x [9], and of SO_2 and NO_x. Liu et al. [10] used an $O_2/H_2O/H_2O_2$ system activated by vacuum ultraviolet (VUV) in a wet VUV spray reactor for the simultaneous removal of NO and SO_2. This hybrid system exhibited good simultaneous removal performance for NO and SO_2. The effects of different process variables on the removal of NO and SO_2 were also investigated. The VUV power, acidity, and alkalinity of the solution, in addition to O_2 and H_2O_2 concentrations, were found to affect the removal of NO from the exhaust, with this study providing a sufficient research foundation for future studies of this technology. In addition, promising and eco-friendly integrated processes involving adsorption, photolysis, and photocatalysis to remove low concentrations of gaseous pollutants from the air have been investigated. Generally, carbon materials, zeolites, and metal–organic framework (MOF) materials are used as adsorbents or carriers in these hybrid systems, while TiO_2 is used as a photocatalyst [7].

However, it should be noted that the NO_x from diesel vehicles' exhaust exceeds 80% of the total gas emitted from gasoline vehicle exhaust. Therefore, controlling the emissions of NO_x from diesel vehicles has become one of the main issues that need to be addressed. At present, post-treatment technology is the most effective method for controlling NO_x emissions [11]. From the perspective of economic and technological feasibility for diesel vehicles' aftertreatment systems, SCR technology is the most suitable choice for controlling diesel vehicle exhaust emissions. Among SCR technologies, NH_3-SCR is the most effective emissions control technology [12,13], wherein the design and preparation of highly efficient catalysts that can effectively utilize NH_3 to remove NO_x are crucial [14]. At present, the catalysts for the NH_3-SCR reaction have been extensively studied [15,16]. SCR catalysts can be classified into categories based on their active components: noble metal catalysts [17,18],

metal oxide catalysts [19,20], and transition metal ion exchange zeolite catalysts [21]. Noble metal catalysts exhibit satisfactory low-temperature performance, but they are expensive, exhibit a narrow operating temperature window, and their poor sulfur resistance limits their widespread application [22]. The transition metal ion exchange zeolite catalysts exhibit a wide operating window at a high NO conversion and poor low-temperature catalytic activity. However, with the international regulations on diesel vehicle pollutant emissions, there are certain constraints on the NO_x gases that are generated under cold-start diesel-engine conditions, and the SCR performance at low temperatures is receiving increased research attention. Therefore, metal oxides have become a focus of research due to their advantages of being cheap, as well as exhibiting high thermal stability and excellent low-temperature catalytic activity. Among the metal-oxide catalysts, traditional V_2O_3–WO_3/TiO_2 catalysts that exhibit satisfactory catalytic performance at 300–450 °C have been commercialized for many years [23]. In addition to the V_2O_3–WO_3/TiO_2 catalysts, metal-oxide catalysts, such as Mn-based oxides, have received increasing research attention due to their diverse valence states and excellent low-temperature SCR activity, and exhibit a good research future in the field of low-temperature denitration. Iron-based catalysts are also cheap, environmentally friendly, and exhibit excellent redox properties and good denitration activity. In addition, Ce- and Cu-based catalysts are widely used in NH_3-SCR reactions. This review provides an in-depth introduction to SCR and the application and role of metal oxides, such as V-, Mn-, Fe-, Ce-, and Cu- oxides, in SCR reactions. Moreover, the development and issues associated with the metal oxides used in the SCR reactions are also summarized.

2. The Main Reactions of the NH_3-SCR System

The NH_3-SCR technology is currently the most popular technology used for removing NO_x from vehicle exhaust. The main reaction of NH_3-SCR is shown in Equation (1), wherein NH_3 reduces NO to H_2O and N_2, which is referred to as the "standard SCR" reaction. When the content of NO_2 increases and reaches the same molar equivalent as NO, the "fast SCR" reaction (Equation (2)) occurs, which was first proposed in the early 1980s and can improve the denitration efficiency at low temperatures as the reaction rate of the "standard SCR" is much lower than that of the "fast SCR". [24]. And excess NO_2 may partially depend on the relatively slow "NO_2-SCR" reaction (Equation (3)) [25]. Moreover, other reactions that occur during the SCR reaction can affect the overall activity and selectivity of the NH_3-SCR catalyst, including NO and NH_3 oxidation (Equations (4) and (5)) and N_2O generation (Equation (6)). Also, N_2O is more likely to contribute towards greenhouse effects than carbon dioxide [26–28].

In diesel exhaust gas, the NO content is much higher than that of the NO_2. However, it is possible to improve the upstream oxidation catalyst to increase the content of NO_2 entering the SCR device, promoting the reduction of NO_x in the presence of NO and NO_2, that is, "fast SCR." The "fast SCR" reaction at low temperatures exhibits higher reaction activity than the "standard SCR" reaction, which can effectively improve the NO_x removal efficiency. According to Equations (1) and (2), it can be inferred that the adsorption of NH_3 and NO/NO_2 on the surface of the SCR catalyst as well as the adsorption and activation of oxygen are important determining factors in the SCR reaction.

$$4NO + 4NH_3 + O_2 \rightarrow 4N_2 + 6H_2O \quad (1)$$

$$NO + 2NH_3 + NO_2 \rightarrow 2N_2 + 3H_2O \quad (2)$$

$$8NH_3 + 6NO_2 \rightarrow 7N_2 + 12H_2O \quad (3)$$

$$2NO + O_2 \rightarrow 2NO_2 \quad (4)$$

$$4NH_3 + 5O_2 \rightarrow 4NO + 6H_2O \quad (5)$$

$$2NH_3 + 2NO_2 \rightarrow N_2 + N_2O + 3H_2O \quad (6)$$

3. SCR Catalysts

3.1. V-Based Catalysts

V_2O_5–WO_3/TiO_2 is the earliest-known commercial NH_3-SCR catalyst, which has a sufficient number of acidic sites, good redox ability, and exhibits high NH_3-SCR catalytic activity in the medium-temperature range (300–450 °C) [29]. However, the exhaust emissions of diesel vehicles contain SO_2, which is easily oxidized to SO_3. NH_4HSO_4 is then formed as a result of the reaction between NH_3 and SO_3, which can deposit on the catalyst surface and cover the active sites, which is the reason for sulfur poisoning of the V_2O_5–WO_3/TiO_2 catalyst (Figure 1) [30]. In addition, the catalyst is also unstable at high temperatures; it may be due to the TiO_2 transformation from anatase to rutile at high temperatures and the separation or volatilization of vanadium species. Therefore, many researchers have turned their attention to the modification of V-based oxide catalysts to address the above issues [31,32].

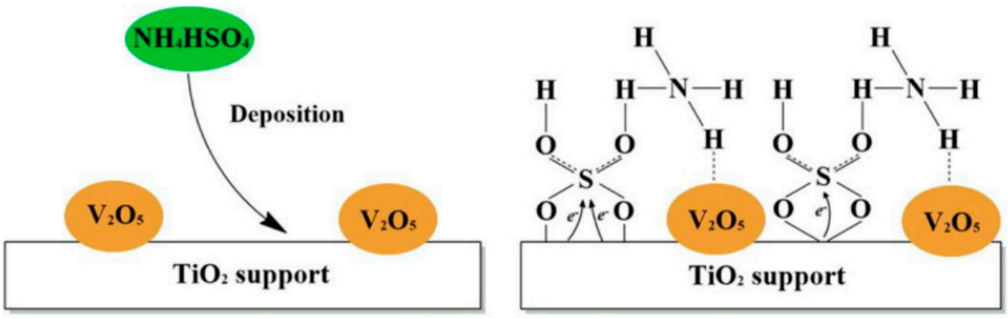

Figure 1. Surface species over V_2O_5/TiO_2 modified by NH_4HSO_4 depositions. Reprinted with permission from Ref. [30]. Copyright 2016, Elsevier B.V.

The addition of active components is an appropriate method to enhance the sulfur resistance of a catalyst and promote its high-temperature stability. A V_2O_5/TiO_2 catalyst modified using Sb has been shown to exhibit high SO_2 tolerance in an NH_3-SCR reaction. Xu et al. [33] also reported a V_2O_5–Sb_2O_3/TiO_2 monolithic catalyst for the NH_3-SCR reaction, the operating temperature window of which was 225–375 °C when the NO_x conversion was >90%. The low-temperature activity of the catalyst significantly decreased after the introduction of SO_2, which was caused by the deposition of NH_4HSO_4. The catalyst modified with Sb_2O_3 promoted the reaction between NH_4HSO_4 and NO, reducing the deposition of NH_4HSO_4, and therefore exhibited better NH_3-SCR performance than the non-modified catalyst in the presence of SO_2. Moreover, a Nb-modified V_2O_5–WO_3/TiO_2 catalyst was also studied for the NH_3-SCR. It was shown that the SO_2 conversion in the presence of the Nb_2O_5–V_2O_5–WO_3/TiO_2 catalyst was the lowest (0.6%) of the tested catalysts at 350 °C at a Nb_2O_5 loading of 2%, while the NO_x conversion was still >95% (Figure 2A). This was because the surface area of the catalyst decreased upon the introduction of Nb, resulting in a decrease in the amount of SO_2 adsorbed. Moreover, the adsorbed oxygen on the catalyst was also significantly reduced after the modification of Nb, indicating that the redox performance of the modified catalyst is weakened, which limited the oxidation of SO_2 [34]. Jung et al. [35] also studied the effects of doping Nb on the NO_x removal from the exhaust in V_2O_5–WO_3/TiO_2 (VWT) catalysts. The results indicated that Nb enhanced the low-temperature performance of the VWT catalyst. Doping of the VWT catalyst with Nb also enhanced its SO_2 and H_2O resistance. After catalyst poisoning for 24 h, the NO conversion of the Nb-doped VWT catalyst at 240 °C was 12% higher than that of the VWT catalyst. This is because, compared to VWT, less ammonium bisulfate (ABS) is formed in

the V_2O_5–WO_3–Nb_2O_5/TiO_2 catalyst. In addition, the V_2O_5/WO_3–TiO_2 catalyst modified with Zr showed better performance than the unmodified catalyst after hydrothermal aging of the catalysts, which was attributed to the inhibition of the shrinkage of the catalyst surface area and the growth of the TiO_2 crystal size upon addition of Zr [36]. Kang et al. [37] physically mixed V_2O_5–WO_3/TiO_2 and several Fe_2O_3 samples with different textural properties for the NH_3-SCR. In the presence of SO_2, the physically mixed catalyst showed higher catalytic stability and SO_2 resistance compared with the V_2O_5–WO_3/TiO_2 catalyst. The V_2O_5–WO_3/TiO_2 catalyst modified by Fe_2O_3 showed relatively stable catalytic performance and high SO_2 resistance. As shown in Figure 2B, Fe_2O_3 effectively prevented catalyst deactivation by inhibiting the formation of ammonium sulfate species. Moreover, Fe_2O_3 also increased the number of acidic adsorption sites of the reactants. In addition, compared to commercial V-based catalysts, the physical mixing of alumina and V-based catalysts resulted in better stability during the SO_2 aging process. This is because the ABS formed on the surface of alumina is obtained through physical contact and migration rather than the direct adsorption of gaseous SO_2. The mixed alumina still exhibited excellent ABS affinity and stability after undergoing SO_2 aging and regeneration processes, which was attributed to its physicochemical properties, such as acidity and pore size [38]. In addition, Ni et al. [39] reported that Ce improved the SO_2 resistance of a V_2O_5–WO_3/TiO_2 catalyst in a low-temperature NH_3-SCR reaction. The ABS on the surface of the catalyst preferentially deposited on CeO_2 to form cerium sulfate, which protected the active species V_2O_5 and TiO_2, maintaining better NH_3-SCR performance in the presence of SO_2. Also, it has been reported that CeO_2 promotes the decomposition of ABS [40]. Wang et al. [41] tested the activity of MO_x–WO_3/TiO_2 catalysts (M = Fe, Mn, Cu, V) treated with SO_2 at 200 °C for 24 h. The results showed that the low-temperature activity of the catalyst significantly decreased after treatment under an SO_2 atmosphere. The catalyst treated with SO_2 inhibited the adsorption of NH_3 and NO on the surface of the catalysts, which was the main reason for its deactivation. Among the prepared catalysts, FeO_x–WO_3/TiO_2 was found to be the best catalyst for the NH_3-SCR at medium to low temperatures due to the easy decomposition of sulfates on its surface.

In addition to adding a single component to modify V-based catalysts, dual component addition can further improve the SCR performance of a catalyst. The Ce and Sb co-modification of a V_2O_5/TiO_2 catalyst was shown to improve SO_2 and H_2O resistance. At a NO_x conversion of >90%, its operating temperature window was 220–450 °C. The excellent catalytic performance of the modified catalyst was attributed to its strong adsorption of NO, large number of acidic sites, and low SO_2 adsorption capacity [42]. Cao et al. [43] reported a Ce^{4+} and Zr^{4+} co-doped V_2O_5–WO_3/TiO_2 catalyst. The addition of Ce and Zr promoted the removal of NO_x at 300–400 °C and showed the best $H_2O + SO_2$ resistance owing to the resulting catalyst having more acidic sites as well as exhibiting strong water and sulfur resistance (Figure 2C). In addition, the promotional effects of Cu and Fe on the V_2O_5–WO_3/TiO_2 catalyst for the removal of NO by NH_3 in the temperature range of 280–360 °C were also studied by Wang et al. [44]. They reported that the addition of Cu led to an increase in the Cu^{2+} content of the catalyst, which is the main species of Cu-containing catalysts, while Fe formed $FeVO_4$ with V. The addition of Cu or Fe improved the SCR performance of the catalyst, which was attributed to a good dispersion of active substances, good redox performance, and abundant active oxygen species.

In addition, the high-temperature instability of V-based catalysts can be improved through doping with Si. The addition of SiO_2 to a WO_3–TiO_2 support improves the resistance of the catalyst to hydrothermal aging. As shown in Figure 2D, the introduction of SiO_2 inhibits the phase transition of TiO_2, the growth of TiO_2 crystal size, and the shrinkage of the catalyst surface area [45]. Similarly, Shao et al. also reported that a Si-doped V_2O_5–WO_3/TiO_2 catalyst showed higher thermal stability than a V_2O_5–WO_3/TiO_2 catalyst as Si doping prevents the anatase to rutile phase transition and contributes to good dispersion of VO_x and WO_3 [46].

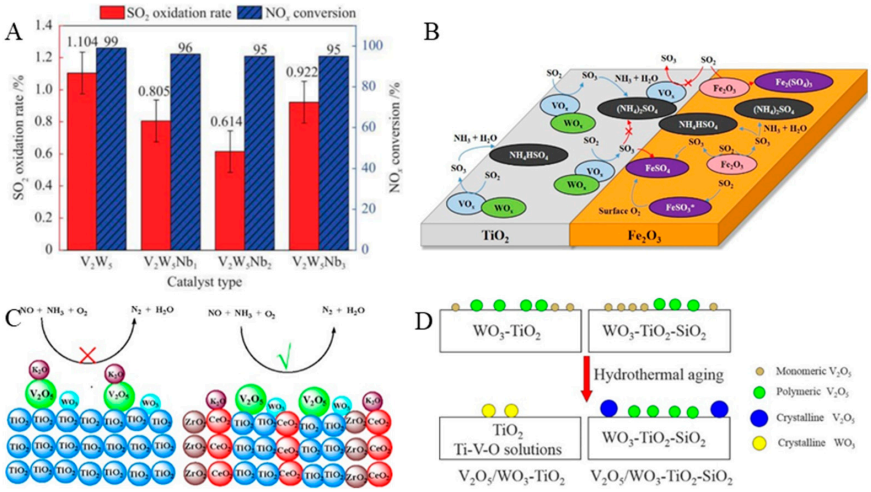

Figure 2. (**A**) Catalytic performance of various catalysts in the simultaneous denitration and SO_2 oxidation at 350 °C. Reprinted with permission from Ref. [34]. Copyright 2022, Elsevier B.V. (**B**) Effects of Fe_2O_3 on V_2O_5-TiO_2 catalyst. Reprinted with permission from Ref. [37]. Copyright 2021, Elsevier B.V. (**C**) The effects poisoning of Ce^{4+} and Zr^{4+} doping. Reprinted with permission from Ref. [43]. Copyright 2017, Elsevier B.V. (**D**) The effects of SiO_2 doping. Reprinted with permission from Ref. [45]. Copyright 2016, Elsevier B.V.

Based on the above research, V-based catalysts have been improved and optimized, achieving significant results. Table 2 shows a good catalytic performance of V-based catalysts for the NH_3-SCR reaction that has been reported in the literature. However, there are still some issues with using V-based catalysts, such as low SCR activity at low temperatures, a narrow activity temperature window, and biological toxicity. Therefore, V-free catalysts are receiving increased research attention.

Table 2. The catalytic performances of V-based catalysts for NH_3-SCR reaction in reported the literature.

Catalysts	Feed Composition					GHSV (h^{-1})	Conversion (Corresponding Temperature Window)	Ref.
	NO (ppm)	NH_3 (ppm)	O_2 (vol%)	SO_2 (ppm)	H_2O (vol%)			
V_2O_5-Sb_2O_3/TiO_2 monolithic catalyst	1000	1000	5	1000	10	5000	>90% (225–375 °C)	[33]
V1WT	500	500	5	-	-	120,000	>90% (300–500 °C)	[36]
VW/Ti + Fe	1200	1200	13	5%CO_2	5.2	120,000	>95% (300–400 °C)	[37]
7Ce-VW/Ti	500 500	500 500	5 5	- 200	- 5.5	160,000	100% (250–400 °C) 65% (250 °C)	[39]
3V6Mo10CeTi	1000	1000	8	-	-	30,000	97% (200 °C)	[40]
SbV10Ce/TiO_2	800 800	800 800	3 3	- 800	- 6	60,000	>90% (220–450 °C) >85% (220–500 °C)	[42]
VWTCZ	500 500	500 500	5 5	- 100	- 5	60,000	>97% (300–400 °C) 75% (350 °C)	[43]
VWTS	500	500	5		10	100,000	>80% (350–550 °C)	[45]
$VWTSi_{10}$-550 °C	500	500	5			300 mL min^{-1}	>80% (205–520 °C)	[46]

3.2. Mn-Based Catalyst

Manganese oxide (MnO_x) catalysts exhibit excellent low-temperature SCR catalytic performance (Table 3) due to their various valence states and good redox capabilities. Therefore, the study of MnO_x has attracted widespread attention. The SCR catalytic activity of MnO_x is related to the valence, specific surface area, and crystallinity of the manganese. Among these attributes of manganese, the crystalline structures of MnO_2 catalysts feature structural defects, and therefore the SCR activity of MnO_2 is higher compared to that of other oxidized forms of manganese [47,48]. Thirupathi et al. [49] showed that the reducibility of MnO_2 catalysts was improved and their NH_3-SCR catalytic performance also was enhanced, indicating that MnO_2 is the active component with the highest SCR reaction activity. Moreover, MnO_x, which exhibits low crystallinity, shows good low-

temperature performance. In addition, the catalytic performance of MnO_x catalysts can be improved by adjusting their crystal structure and morphology. Yang et al. [50] adjusted the crystal phase of MnO_x to enhance the denitration performance and found that α-MnO_2 exhibited better catalytic activity compared to β-MnO_2, γ-MnO_2, and δ-MnO_2. Meanwhile, the morphology of the catalyst also affects its redox properties. Liang et al. [51] introduced W and Mo as new acidic centers into α-, β-, γ-, and δ-MnO_2. When Mn–O–W or Mn–O–Mo bonds formed on the surface of α-MnO_2, the best ability to capture NH_3 and NO on the surface of the catalyst was observed. The results showed that the high activity of MnO_2 is related to the strong interaction between H and the surface O_{2c} site and that this site is prone to forming oxygen vacancies.

Moreover, the type of MnO_x and the valence state of Mn play crucial roles in the SCR reaction [52,53]. The SCR catalyst activity of MnO_x varies according to the valence state. It has been reported that MnO_2 exhibits the best SCR catalytic performance, which is related to Mn^{4+} promoting the redox cycle and enhancing the oxidation of NO to NO_2 [54,55]. Zhan et al. [56] prepared ordered mesoporous MnO_2 and Mn_2O_3 using the KIT-6 template (Figure 3A). The mesoporous manganese oxide has more chemically adsorbed oxygen and stronger acid sites, as well as strong reducibility. As shown in Figure 3B, mesoporous MnO_2 removed NO with an efficiency of 100% in the temperature range of 150–250 °C, which was higher than the activity of mesoporous Mn_2O_3 due to mesoporous MnO_2 having more Mn^{4+}. The results indicate that the mesoporous structure and oxidation state of MnO_x have a major impact on the SCR. Liu et al. [57] constructed MnO_2 nanosheets with a large number of oxygen vacancies via a solvent-free synthesis method, which exhibited the best low-temperature activity among tested samples, with a denitration efficiency of ≤100% at 100 °C (space velocity 700,000 h^{-1}) (Figure 3C). Moreover, the NH_3-SCR mechanism of the MnO_2 nanosheet catalyst was further studied and the results showed its catalysis to be underpinned by the Langmuir–Hinshelwood (L–H) mechanism. Hollow spherical MnO_2, Mn_2O_3, Mn_3O_4, and MnO catalysts of similar sizes were obtained by decomposing $MnCO_3$ in air at 440 and 500 °C, and under H_2 and Ar at 430 °C, respectively. Within different reaction temperature ranges, as shown in Figure 3D, the SCR performance order of the MnO_x catalysts was different and the NO conversion of MnO_2 was the highest [58].

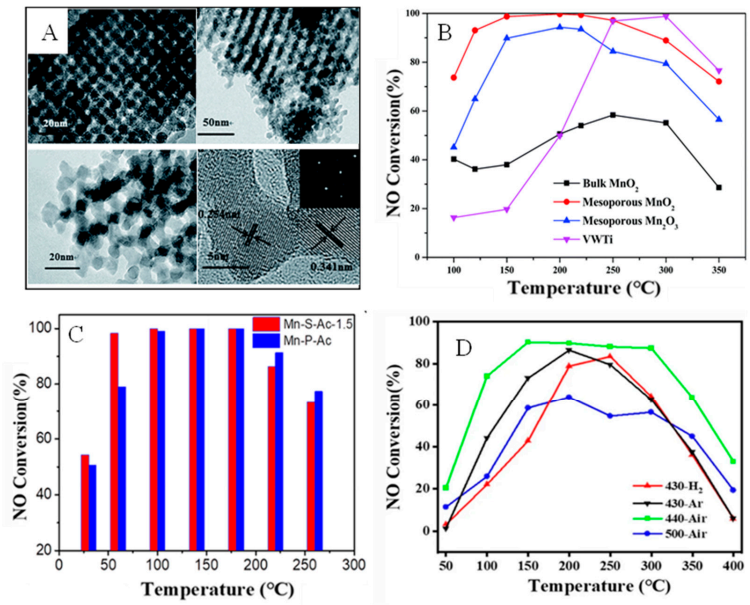

Figure 3. (**A**) The TEM images of MnO_x. Reprinted with permission from Ref. [56] Copyright 2015, The Royal Society of Chemistry and (**B**–**D**) NO conversion of MnO_x in different published literature. (**B**) Reprinted with permission from Ref. [56]. Copyright 2015, The Royal Society of Chemistry. (**C**) Reprinted with permission from Ref. [57]. Copyright 2018, American Chemical Society, and (**D**) Reprinted with permission from Ref. [58]. Copyright 2022, Springer).

However, undoped MnO_x catalysts exhibit a narrow temperature window for the NH_3-SCR, as well as low N_2 selectivity and SO_2 resistance, which limit their practical applications [59,60]. Therefore, doping or mixing MnO_x with other metal oxides can greatly improve their SCR activity and SO_2 resistance due to the interaction between the Mn and doping element [61,62]. Table 3 summarizes the catalytic performances of Mn-based catalysts for the NH_3-SCR reaction reported in the literature.

CeO_2 can store and release oxygen and is added to Mn-based oxides as a promoter to enhance the performance and SO_2 resistance of catalysts in the SCR reactions. After the introduction of Ce, SO_2 preferentially reacts with Ce to form cerium sulfate, which acts as a sacrificial site to reduce the sulfation of MnO_x, thereby improving the sulfur resistance of the catalyst. Jin et al. [63] studied the mechanism of sulfur poisoning in Mn–Ce composite oxides in detail. As shown in Figure 4A, the introduction of Ce inhibits the generation of manganese sulfate on the surface of the catalyst. Moreover, it has been reported that CeO_2 can store NO_x as a SO_2 trap to prevent sulfation of the active sites when SO_2 is exposed [64,65]. Chen et al. [66] studied the SCR performance of doped CeO_2 catalysts. The results showed that the NO conversion of the catalysts doped with different crystal forms of MnO_x and CeO_2 was always >95% in the range of 75–250 °C, indicating that MnO_2-doped CeO_2 catalysts have excellent low-temperature NH_3-SCR performance. In addition, catalysts doped with CeO_2 also produce less N_2O and the generated N_2O mainly arises from the SCR reaction rather than NH_3 oxidation. This is because compared with an undoped manganese oxide catalyst, the reduction and acidity of the catalyst doped with CeO_2 are improved, which is conducive to the adsorption of NH_3 and NO, and reduces the reactivity of O_2 and NH_3.

In addition, different Mn and Ce contents also affect the catalytic performance of the NH_3-SCR. Wang et al. [67] studied the SCR catalytic performance of Mn_4CeO_x and $MnCe_4O_x$ catalysts, reporting that the Mn_4CeO_x catalyst exhibited higher catalytic activity than the $MnCe_4O_x$ catalyst in the temperature range of 75–250 °C and that the NO_x removal of the Mn_4CeO_x catalyst was 100% at 150 °C. Within the tested temperature range, the N_2 selectivity of the Mn_4CeO_x catalyst was always higher than that of the $MnCe_4O_x$ catalyst due to the Mn_4CeO_x catalyst exhibiting better redox capacity and stronger acidity. Moreover, the relative content of Ce^{4+} in the Mn_4CeO_x catalyst was relatively high, indicating that it produces more Mn^{4+} and generates more oxygen vacancies, thereby promoting the SCR reaction.

The rare earth metal Sm is also a good dopant, as it is non-toxic, cheap, stable, and can control the chelation of transition state intermediates [68]. Meng et al. [69] first discovered that the doping of Sm enhanced the sulfur and water tolerance of MnO_x catalysts. Moreover, Chen et al. [70] revealed the promotional effects of Sm doping on the denitration and sulfur resistance of a Sm-doped $MnFeO_x$ catalyst, the results of which are shown in Figure 4B. The strong electron transfer between Sm^{2+} and Mn^{4+} preferentially induced Fe and Sm to act as sacrificial sites to react with SO_2, effectively suppressing the formation of metal sulfates and ammonium salts on the catalyst surface. In addition, adding transition-metal oxides to MnO_x also enhances the catalytic performance of the catalysts. Li et al. [71] prepared cobalt-doped MnO_x catalysts via a coprecipitation method. The catalyst with a Mn/Co = 1 exhibited the best catalytic activity, with a NO conversion of >90% at 100–275 °C. The doping of MnO_x with Co greatly increased the high-valence-metal ion content and chemically adsorbed oxygen on the surface of the MnO_x catalyst and reduced the apparent activation energy of the catalyst, which contributed to the excellent SCR catalytic performance of the catalyst. Ni-doped MnO_x catalysts also showed good results in the NH_3-SCR; it is related to the synergistic effect between Mn and Ni. As shown in Figure 4C, Ni^{3+} traps electrons from Mn^{3+} and they are converted into Ni^{2+} and Mn^{4+}, respectively. The activation process of converting Mn^{3+} to Mn^{4+} is related to the dehydration of NH_3 to NH_2, which helps to improve SCR activity and the stability of Ni–MnO_x catalysts. According to the reaction $Mn^{3+} + Ni^{3+} \leftrightarrow Mn^{4+} + Ni^{2+}$, Ni^{3+} converts to Ni^{2+}, with the generated Ni^{2+} providing electrons to O_2 before reverting back to Ni^{3+}. Finally, NH_2 and O^{2-} react with NO gas to

produce non-polluting products (Figure 4C) [72]. Li et al. [73] also reported Co-, Ni-, and Cu-doped MnO_x catalysts for the SCR, and it was found that it was easier to use Co to produce Mn-enriched oxides, with Co–MnO_x exhibiting the highest NO_x removal activity and SO_2 resistance among the synthesized catalysts. The high activity of Co–MnO_x contributes to its special Mn-enriched surface $(Co^{2+})_{tet}(Mn^{3+}Co^{3+})_{oct}O_4$ structure. In addition, Co–MnO_x exists in lower density surrounding the Mn. Meanwhile, Co–MnO_x benefits from the electron transfer between Mn and Co, and surface nitrate can react with the adsorbed NH_3 using the L–H mechanism (Figure 4D).

Based on the above research, Mn-based catalysts exhibit excellent low-temperature catalytic performance, but the N_2 selectivity and water/sulfur resistance at high NO conversion still need to be further improved. In addition, the reaction mechanism of Mn-based catalysts should be further studied.

Table 3. The catalytic performances of Mn-based catalysts for NH_3-SCR reaction in reported the literature.

Catalysts	Feed Composition					GHSV (h^{-1})	Conversion (Corresponding Temperature Window)	Ref.
	NO (ppm)	NH_3 (ppm)	O_2 (vol%)	SO_2 (ppm)	H_2O (vol%)			
MnO_2 Mn_2O_3 Mn_3O_4	500	500	11			36,000	100% (150 °C) 100% (250 °C) 100% (200 °C)	[48]
Mn–Ni/TiO_2 (Ni/Mn = 0.4)	400	400	2	-	--	50,000	100% (200 °C)	[49]
α-MnO_2 γ-MnO_2 β-MnO_2	500	500	19	-	-	36,000	100% (120 °C) 100% (120 °C) 40% (120 °C)	[50]
mesoporous MnO_2	500	500	3	-	-	28,000	100% (150–250 °C)	[56]
$Mn_3CeW_{0.3}O_x$	500 500	500 500	5 5	-	- 5	100,000	>70% (100–275 °C) >72% (150–300 °C)	[59]
Cr(0.4)–MnO_x	1000 1000	1000 1000	3 3	- 100	-	30,000	>98% (120–220 °C) 85% (120 °C)	[61]
CeO_2@α-MnO_2	500	500	11	-	-	36,000	100% (75–250 °C)	[66]
SmMnFe-0.1	500 500	500 500	5 5	100	5	60,000	100% (75–200 °C) 90% (200 °C)	[70]
Ni(0.4)-MnO_x	500 500	500 500	5 5	100		64,000	100% (150–240 °C) 87% (230 °C)	[72]
Co-MnO_x	500	500	5	200	10	32,000	86% (200 °C)	[73]

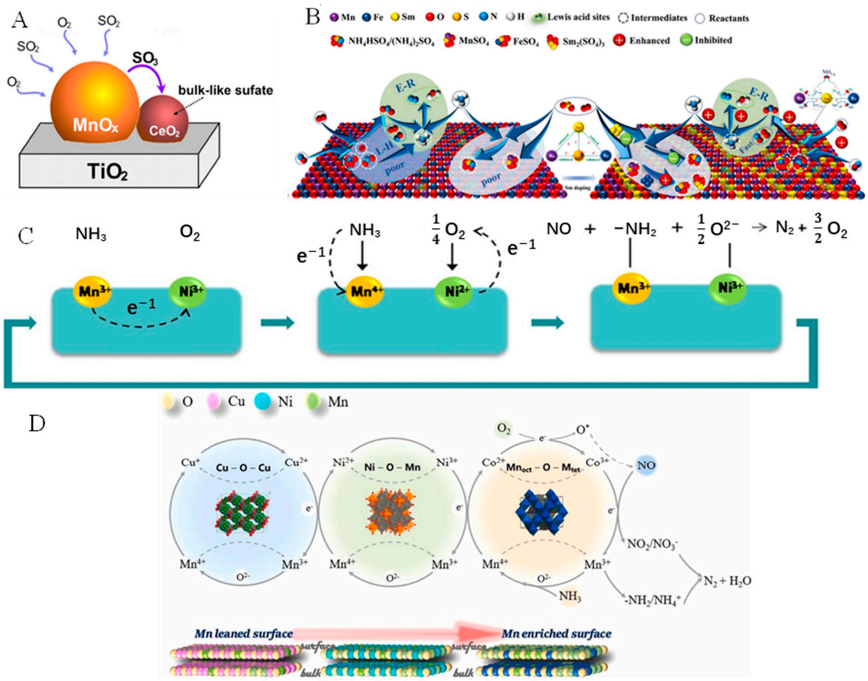

Figure 4. (**A**) The formation pathway of bulk-like sulfate on Mn-Ce/TiO_2 samples. Reprinted with permission from Ref. [63]. Copyright 2014, Elsevier B.V. (**B**) Mechanism model of Sm promoting SCR activity and SO_2 resistance over $MnFeO_x$ catalysts. Reprinted with permission from Ref. [70]. Copyright

2022, Elsevier B.V. (**C**) The electrons transfer between Mn ions and Ni ions over the catalyst for NH_3-SCR. Reprinted with permission from Ref. [72]. Copyright 2014, Elsevier B.V. and (**D**) The proposed mechanism of the SCR reaction over the Ni(0.4)-MnO_x catalyst and the synergetic catalytic effect between Mn and Ni cations. Reprinted with permission from Ref. [73]. Copyright 2021, Elsevier B.V.

3.3. Fe-Based Catalysts

The catalytic effect of Fe_3O_4 and FeO is very weak for the SCR, so Fe-based catalysts are generally based on Fe_2O_3 as the main active substance. In recent years, Fe_2O_3 has attracted attention in the field of developing Fe-based SCR catalysts due to its excellent redox properties, acidity, and sulfur resistance [74]. The conversion of the valence state of iron in iron oxide between Fe^{2+} and Fe^{3+} is helpful for generating lattice oxygen. Fe^{3+} converts NO into NO_3^- and NO_2^-, improving the SCR activity of Fe-based catalysts [75]. Different crystal forms of iron oxide, such as α-Fe_2O_3, β-Fe_2O_3, and γ-Fe_2O_3, exhibit different NH_3-SCR catalytic activities. The α-Fe_2O_3 is more abundant in nature compared to β-Fe_2O_3 and γ-Fe_2O_3, and exhibits low toxicity, high resistance to SO_2, and has a suitable electronic band structure [76]. Zhou et al. [77] reported an $Fe_2(SO_4)_3/CeO_2$ catalyst for NH_3-SCR, which exhibited good NH_3-SCR performance and enhanced N_2O selectivity as a result of the synergetic interaction of Fe, Ce, and SO_4^{2-}. As shown in Figure 5, Yu et al. [78] conducted thermal stability experiments over an $Fe_2(SO_4)_3/TiO_2$ catalyst. It was found that $Fe_2(SO_4)_3/TiO_2$ decomposed into α-Fe_2O_3 at >350 °C, which led to a slight decrease in the number of Brønsted acid sites and NO_x conversion. α-Fe_2O_3 bound gaseous NO_x more effectively than NH_3, resulting in the production of abundant surface nitrate species, which may have had a negative impact on its catalytic performance in the SCR. Therefore, great efforts have been devoted to adjusting the redox properties and surface acidity of α-Fe_2O_3. Cerium oxide is added to Fe oxide due to its unique ability to store and release oxygen, which promotes lattice distortion to generate oxygen vacancies and regulates its chemical and physical properties, such as reducibility and surface acidity, leading to a "fast SCR" that improves the activity of the catalyst at low temperature [79]. Chen et al. [80] prepared an α-Fe_2O_3 with a single-atom Ce-doping catalyst. It was reported that the NO conversion of the $Fe_{0.93}Ce_{0.07}O_x$ catalyst was 93% at 250 °C, which was maintained for 168 h when 200 ppm SO_2 and 5 vol% H_2O were introduced. This can be explained by the doping of Ce in the FeO_x catalyst generating Fe–O–Ce sites, which were beneficial to the NO oxidation of the catalyst and the reduction of NO_x by NH_3, resulting in the high activity of the catalyst. Therefore, the presence of Fe–O–Ce sites in this catalyst is crucial. Meantime, the catalyst also exhibited good resistance to SO_2/H_2O, as the NH_4HSO_4 deposited on the surface by the catalyst decomposes at lower temperatures.

In addition, compared to α-Fe_2O_3, γ-Fe_2O_3 has more surface defects and hydroxyl groups, therefore, improving its adsorption performance for NH_3 [81]. Mou et al. [82] reported that γ-Fe_2O_3 nanorods featuring reactive (110) and (100) crystal planes with iron sites and adjacent oxygen sites can jointly adsorb NO and NH_3. Yu et al. [83] also studied a γ-Fe_2O_3 catalyst regarding its resistance to SO_2. At >300 °C, the NO conversion fell to 50% within the first 3 h. Then, with time, the conversion of NO gradually recovered to approximately 80%. It was speculated that SO_2 may hinder the adsorption of NO_x; the formed surface sulfate can terminate the L–H reaction within the first 3 h, but promotes the Eley–Rideal (E–R) reaction to occur after 3 h. However, the conversion of NO continued to decrease without rebounding at <300 °C. This also means that beneficial reactive surface sulfates may form at a higher temperature. Therefore, different sulfate coverage at different temperatures may be triggered following different reaction mechanisms related to the NH_3-SCR reaction over sulfation catalysts. Moreover, as the balance between acidity and redox performance of the catalyst in the NH_3-SCR reaction is crucial, the doping effects of Ti^{4+}, $Ce^{3+/4+}$, and Al^{3+} were systematically studied due to their different acidity and redox properties [84]. Among the doped catalysts, the catalyst doped with Ti^{4+} exhibited the best catalytic performance, with a four-fold NO_x conversion increase (100 °C) compared

to Fe_2O_3, which is related to its acidity and reducibility. The samples doped with $Ce^{3+/4+}$ exhibited excellent redox properties but had fewer acidic sites. Meanwhile, after the introduction of SO_2 and H_2O, the $Fe_9Ti_1O_x$ catalyst achieved a NO_x conversion of 80% at 250 °C and maintained this performance for 80 h. The excellent water and sulfur resistance of the $Fe_9Ti_1O_x$ catalyst makes it a good candidate catalyst for the SCR reaction. In addition, the sulfation and doping of Ti reduced the oxidation of Fe^{3+} and inhibited NH_3 oxidation. Fan et al. prepared Ti-doped Fe_2O_3 (Ti-Fe_2O_3) nanoparticles [85], which showed a significant NO conversion of 80% at 250 °C under 100 ppm SO_2. The addition of Ti^{4+} resulted in the migration of electrons around Fe^{3+}, leading to electron deficiency in Fe^{3+}. As a result, electron-donating NH_3 was preferentially adsorbed by Fe^{3+}, which is beneficial for enhancing the low-temperature resistance of the Ti-Fe_2O_3 catalyst to SO_2. Moreover, doping of the Fe_2O_3 catalyst with Ti^{4+} resulted in the conversion of a large number of Brønsted acid sites into Lewis acid sites. In addition, a Sm-doped Fe_2O_3 catalyst was successfully prepared via a citric acid assisted sol–gel method. The results showed that the reaction rate of NO_x over the $Fe_{0.94}Sm_{0.06}O_x$ catalyst was almost 11 times that of an undoped Fe_2O_3 catalyst. The $Fe_{0.94}Sm_{0.06}O_x$ catalyst maintained a NO_x conversion of >85% at 250 °C for 168 h after SO_2 and H_2O were introduced. The reason for the high activity and stability of the catalyst in the presence of SO_2+H_2O is that the doping of Sm promoted the decomposition of NH_4HSO_4 on the catalyst surface. [86].

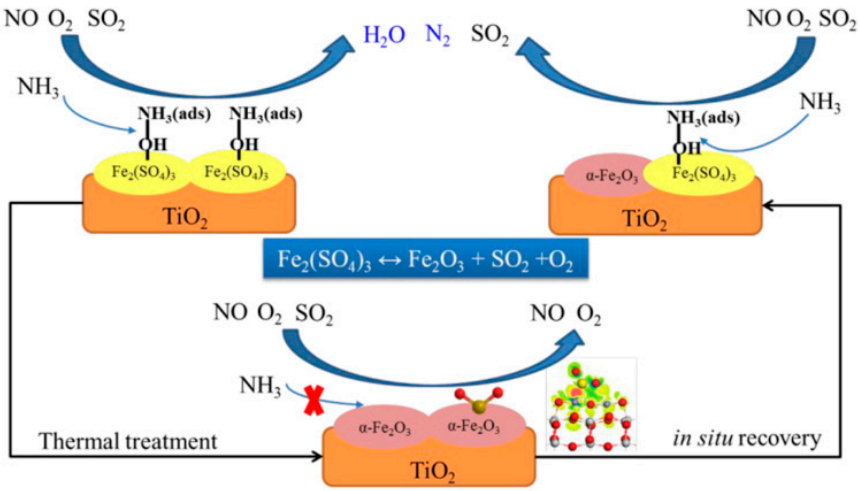

Figure 5. Decomposition of sulfates and in situ recovery on α-Fe_2O_3/TiO_2 catalysts. Reprinted with permission from Ref. [78]. Copyright 2019, Elsevier B.V.

Zhang et al. [87] prepared a Cu-modified W/Fe_2O_3 catalyst, and Fe_2O_3 and Fe_2CuO_z supports were successfully prepared by adjusting the glucose content. The introduction of Cu prevented the growth of γ-Fe_2O_3 crystals and the generation of α-Fe_2O_3 crystals in addition to promoting the formation of highly dispersed $CuFe_2O_4$, which is beneficial for the reaction $Cu^{2+} + Fe^{2+} \leftrightarrow Cu^{+} + Fe^{3+}$, thereby increasing its $O_\alpha/(O_\alpha + O_\beta)$ value and redox properties and exhibiting the best NH_3-SCR catalytic performance based on a large amount of Cu^{+} and Fe^{3+}. Fan et al. [88] also used three-dimensional (3D) hierarchical dandelion-like TiO_2 microspheres and reduced graphene oxide (rGO) as carriers to synthesize Cu/Fe-TiO_2-rGO catalysts for NH_3-SCR that exhibited good catalytic performance. The temperature window of the $Cu_{0.4}Fe_{0.6}$-TiO_2-rGO catalyst at 90% NO conversion was 250–350 °C. Moreover, the presence of Fe species enhanced the activity at a low temperature. In addition, there were a large number of Lewis acid sites and a small number of Brønsted acid sites on the catalyst surface, indicating that the Fe in the catalyst follows the L–H mechanism to promote the removal of NO_x. Moreover, Liu et al. [89] reported a WO_3-doped Fe_2O_3 catalyst for NH_3-SCR. The 10W/Fe catalyst showed excellent catalytic performance, with a temperature window of 275–425 °C when the NO conversion was >90%. This result was attributed to the interaction between WO_3 and Fe_2O_3. The doping of Fe_2O_3 with

WO_3 enhances the acidity of the catalyst and increases its specific surface area, which is conducive to the adsorption of reactants and thus enhances the catalytic performance of the catalyst. The catalytic activity of the catalyst decreased after the introduction of SO_2 and H_2O, which was caused by the deposition of sulfate species. However, after the removal of SO_2 and H_2O from the reaction atmosphere, the catalytic activity recovered, indicating that the catalyst showed high H_2O and SO_2 tolerance. Wang et al. reported [90] that a 30% WO_3–FeO_x catalyst showed high catalytic activity, with 100% NO_x removal between 225 and 500 °C. The introduction of WO_3 promoted Fe_2O_3 to adsorb more oxygen. As shown in Figure 6A, in situ diffuse reflectance infrared Fourier transform spectroscopy (DRIFTS) measurements showed that the introduction of WO_3 increased the number of acidic sites; moreover, it also helped to form adsorbed NO_x species, which explained the enhanced performance of the WO_3-FeO_x catalysts. It was reported that the catalyst followed E–R and L–H mechanisms (Figure 6B). Based on this, adding Ce increased the number of active oxygen atoms and the position of moderate alkalinity. Meanwhile, the addition of W significantly reduced the number of alkaline sites and increased the number of Brønsted acid sites. The addition of Ce and W was beneficial for balancing the surface acidity and alkalinity of the catalyst, which was also the reason why the catalyst exhibited excellent low-temperature SCR activity (Figure 6C) [79]. Kang et al. [91] also prepared Fe_2O_3-modified CeO_2-WO_3 catalysts for NO_x reduction in the presence of SO_2, which exhibited excellent SCR catalytic performance in the range of 270–420 °C. The addition of Fe_2O_3 increased the proportion of Ce^{3+} and the number of surface oxygen vacancies in the catalyst. In addition, after introducing SO_2, the addition of Fe_2O_3 inhibited sulfur poisoning and prevented the irreversible binding of SO_2 with active ingredients, which also explained the good SO_2 resistance of the catalyst.

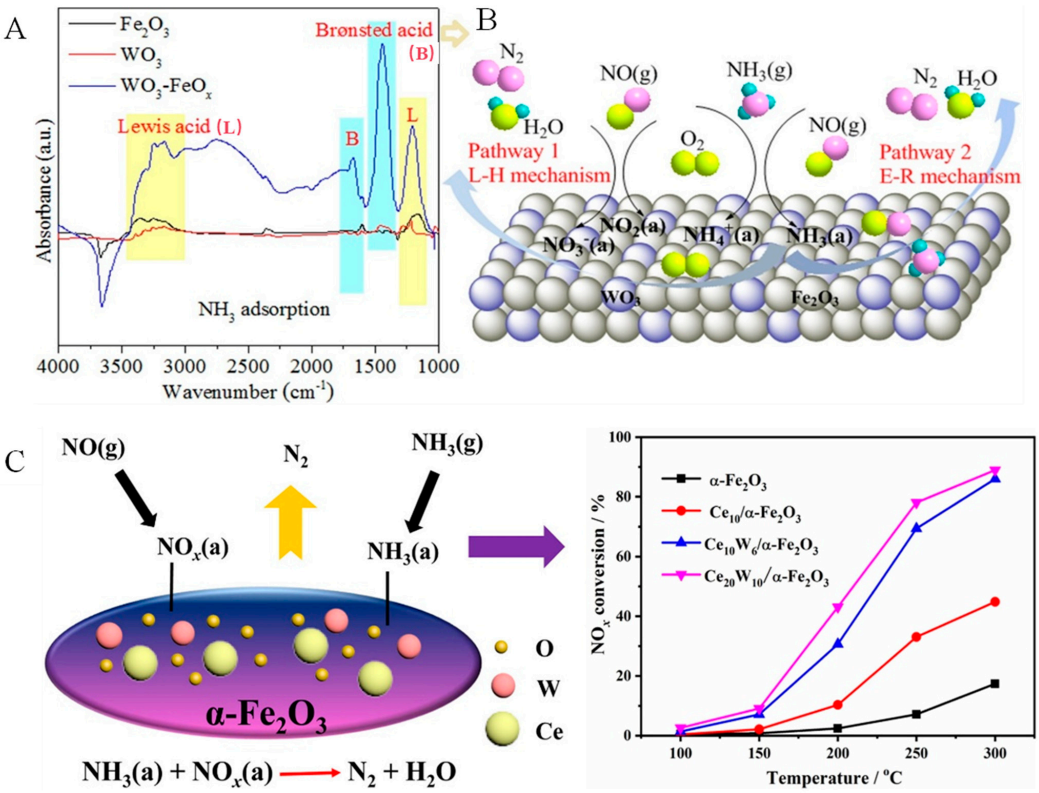

Figure 6. (**A**,**B**) In situ DRIFTS result and reaction mechanism of WO_3-FeO_x catalysts. Reprinted with permission from Ref. [90]. Copyright 2020, Elsevier B.V. and (**C**) The effect of W and Ce doping Fe_2O_3. Reprinted with permission from Ref. [79]. Copyright 2022, Elsevier B.V.

Based on the above research, Fe-based SCR catalysts have been shown to exhibit higher activity at medium to high temperatures, as shown in Table 4, but their low-temperature

activity is not ideal and needs to be further improved. Therefore, modified Fe-based catalysts are particularly important for enhancing low-temperature catalytic performance and N_2 selectivity.

Table 4. The catalytic performances of Fe-based catalysts for NH_3-SCR reaction in reported the literature.

Catalysts	Feed Composition					GHSV (h^{-1})	Conversion (Corresponding Temperature Window)	Ref.
	NO (ppm)	NH_3 (ppm)	O_2 (vol%)	SO_2 (ppm)	H_2O (vol%)			
6FeSCe	500	500	5	-	-	118,000	>90% (300–450 °C)	[77]
	500	500	5	50	5		85% (300 °C)	
FeTi	500	500	4			60,000	>90% (350–450 °C)	[78]
$Fe_{0.93}Ce_{0.07}O_x$	500	500	5	-	-	90,000	>95% (175–325 °C)	[80]
	500	500	5	200	5		93% (250 °C)	
γ-Fe_2O_3-FM	500	500	3	-	-	30,000	96% (230 °C)	[81]
	500	500	3	300			79% (230 °C)	
$Fe_9Ti_1O_x$	500	500	5	-	-	60,000	>80% (150–350 °C)	[84]
$Fe_{0.94}Sm_{0.06}O_x$	500	500	5	-	-	60,000	>95% (175–325 °C)	[86]
	500	500	5	200	5		85% (250 °C)	
10W/Fe	500	500	5	-	-	100,000	>90% (275–425 °C)	[89]
	500	500	5	50	5		90% (350 °C)	
0.3W-Fe	600	600	5			60,000	100% (250–500 °C)	[90]
	600	600	5	100	10		90% (250 °C)	
Fe(4)@CeW/H	500	500	5			40,000	>96% (270–420 °C)	[91]
	500	500	5	100	8		82% (300 °C)	

3.4. Ce-Based Catalyst

Cerium oxide has unique advantages in the NH_3-SCR reactions due to its excellent capacity for storing and releasing oxygen [92,93], good redox performance [94,95], and strong NO_x and NH_3 adsorption capabilities [96,97]. However, undoped CeO_2 catalysts exhibit poor SCR activity and SO_2 resistance at <200 °C. The presence of SO_2 results in the formation of NH_4HSO_4, $Ce_2(SO_4)_3$, and $Ce(SO_4)_2$ on Ce-based catalysts [98]. NH_4HSO_4 blocks the active sites and reduces the activity of the catalysts. $Ce(SO_4)_2$ and $Ce_2(SO_4)_3$ inhibit the formation and adsorption of nitrate, disrupting the Ce^{3+}/Ce^{4+} redox cycle and leading to deactivation of the catalyst, which greatly limits the application of CeO_2 [99,100]. Adding other active components to CeO_2 can effectively resolve these issues. A good interaction between Ce and Mn endows them with good redox properties and denitration performance, as well as sulfur resistance [101,102]. Compared with a single-oxide catalyst, MnO_x–CeO_2 has been shown to exhibit higher activity for NO oxidation, which is due to its higher oxygen mobility and stronger reducibility [103]. Therefore, Ce–Mn composite oxide catalysts have been widely applied for NH_3-SCR reactions. Qi et al. reported, for the first time, that a 30 wt% Mn/70 wt% Ce exhibited excellent SCR activity at low temperatures [104]. Gao et al. [105] synthesized Mn/CeO_2 catalysts and studied their catalytic activity. The results showed that the Mn/CeO_2 catalyst exhibited high activity, with a NO_x conversion of 100% at 150–240 °C. Moreover, it was also reported that Mn–Ce composite oxides exhibited excellent low-temperature SCR catalytic performance, with a temperature window of 150–310 °C at >90% NO_x conversion [106]. It is worth noting that the Mn–Ce composite oxide exhibited good SO_2 resistance, with the NO_x conversion of the catalyst increasing from 92.6% to 97.8% at 150 °C in the presence of 200 ppm SO_2 (Figure 7A). In the presence of SO_2 in the reaction atmosphere, the NH_3 adsorption sites of the active component separated from the oxidant, inhibiting the oxidation of NH_3 (Figure 7B). In addition, a prepared Mn_xCe_y binary catalyst with a 3D network structure also exhibited good catalytic performance, which was attributed to the rich pore structure of the catalyst being conducive to gas diffusion and promoting the NH_3-SCR reaction. Among them, the Mn_1Ce_1 catalyst showed the best denitrification properties, with a NO conversion of 97% at 180 °C [107]. Lin et al. also studied MnO_x-CeO_2/TiO_2 catalysts for the NH_3-SCR reaction, with the catalysts exhibiting excellent low-temperature catalytic performance for the NH_3-SCR due to the large differences in radii; Mn atoms can enter lattice CeO_2 to form

a $MnCeO_x$ solid solution structure, which improved the redox performance of the catalyst. Moreover, the presence of abundant Mn^{4+} and Ce^{3+} on the catalyst surface generated more active oxygen [108].

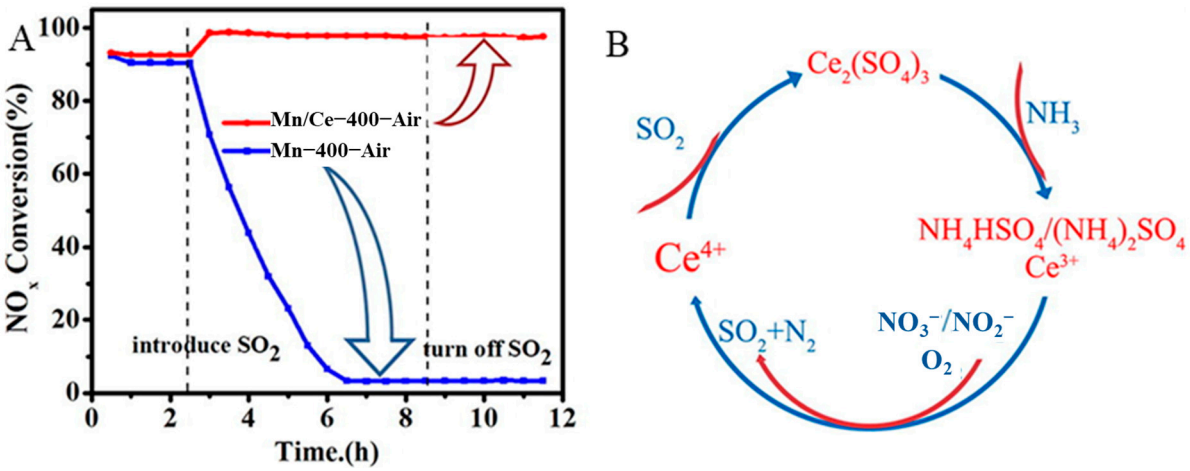

Figure 7. (**A**) NO conversion of MnCe composite oxide catalyst in the presence of SO_2. and H_2O. (**B**) The mechanism of SO_2-poisoning over MnCe composite oxide catalyst. Reprinted with permission from Ref. [106]. Copyright 2021, Elsevier B.V.

In addition to manganese, the doping of the catalysts with other metals can also improve their denitration activities. Wang et al. [109] prepared WO_3/CeO_2 catalysts, which exhibited excellent SCR performance due to the strong interaction between W and Ce. It was also reported that W–Ce composite metal-oxide catalysts loaded with different W/Ce content were prepared via a coprecipitation method, which had a significant impact on the surface acidity, especially the number of Brønsted acid sites, with $W_{0.18}CeO_x$ exhibiting the best NH_3-SCR performance at 190–490 °C for 100% NO_x conversion, while still maintaining a wide active temperature window from 235 to 460 °C when treated with 5% H_2O at high temperature for 12 h [110]. Yao et al. [111] developed TiO_2/CeO_2 nanocubes and nanorods for the effective reduction of NO_x. It was speculated that the strong interaction between the (110) plane of the CeO_2 nanorods and highly dispersed TiO_2 may have contributed to the improvement in the activation and reduction behavior of chemically adsorbed oxygen. Moreover, Liu et al. [112] prepared Co-, Cu-, and Fe-doped Ce-Ti mixed oxides, and improved the low-temperature SCR activity of the catalysts. Among the tested samples, Co-Ce-Ti catalysts exhibited the best SCR activity and the widest temperature window at low temperatures. This may be due to the different ionic sizes of Co^{2+} and Ce^{4+}, which greatly promote the lattice distortion of Ce-Ti mixed oxides. Subsequently, the proportion of Ce^{3+} to surface adsorbed oxygen increased, which was conducive to the generation of adsorbed NO_x species and to improving the L-H reaction. Meanwhile, the coordination of unsaturated cation sites on the Co-Ce-Ti samples induced the adsorption of more NH_3 at Lewis acid sites. It is considered to be key in the E-R mechanism, thereby promoting a reaction that follows the E-R mechanism. The enhancement in the reaction via the L-H and E-R mechanisms seemed to be directly related to an improvement in the denitration performance of the Co-Ce-Ti samples, and the L-H mechanism at low temperatures may have been the main mechanism due to its fast reaction rate (Figure 8). In addition, Ce-Cu composite oxides have attracted research attention due to the interaction of Ce and Cu in the oxidation reaction. However, even during mild heat treatment, deactivation of Ce-Cu composite oxides may occur. This deactivation may be due to the high migration rate over Cu and the sensitivity of CeO_2 to thermal damage, leading to the formation of Cu_xO_y clusters [113,114]. Therefore, developing more heat-resistant Ce-Cu composite oxides is the most important step in the application of CeCu composite oxides in the SCR processes [115–117]. In further research, among the Co-, Mn-, and Cu-modified Ce-W-Ti

catalysts, the temperature range of Cu/Ce-W-Ti catalysts with 5 wt.% Cu was 260–400 °C at a NO_x conversion of >90%. The catalysts also exhibited higher SO_2 and water vapor resistance, which may be attributed to the highly dispersed Cu species, in addition to the higher Ce^{3+} and active oxygen contents of the catalysts [118]. In addition, Li et al. [119] reported novel ternary CeNbVO catalysts for NH_3-SCR. The prepared CeNbVO catalysts exhibited high NH_3-SCR activity, where among them the temperature window of CeNbVO-2 was 210–420 °C for a NO conversion of >90%. The excellent catalytic performance of the catalyst was attributed to its appropriate acidity and redox properties. Moreover, this catalyst showed better H_2O/SO_2 resistance than the other tested catalysts.

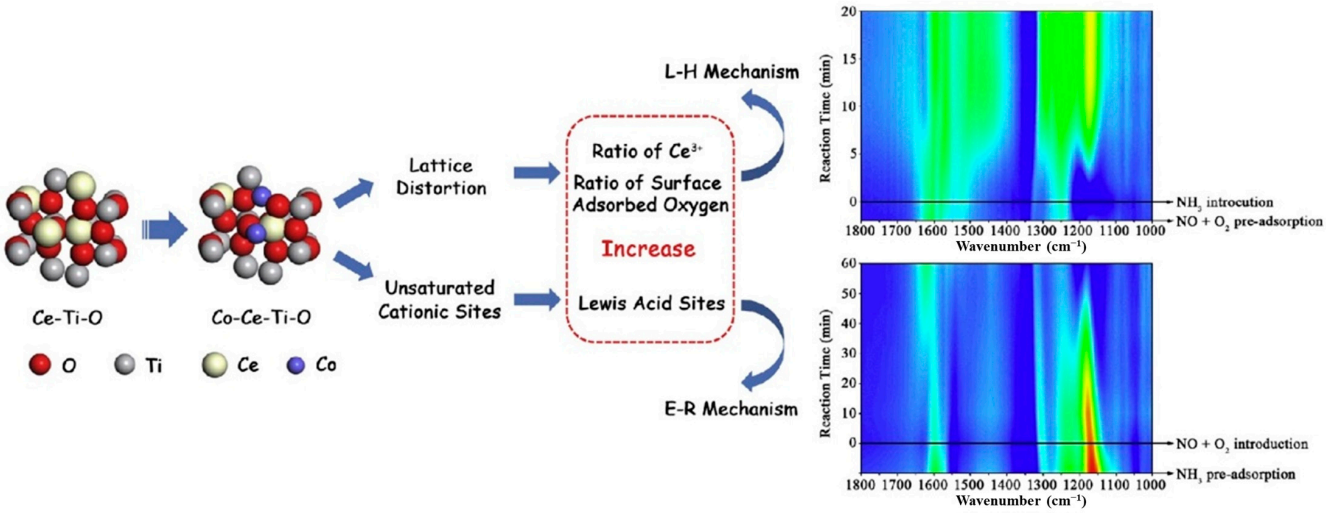

Figure 8. The effect of Co over Co-Ce-Ti catalyst on the E-R and L-H mechanism. Reprinted with permission from Ref. [112]. Copyright 2017, Elsevier B.V.

Based on the above research, progress has been made in the study of Ce-based catalysts for NH_3-SCR. Among them, Mn-Ce composite oxide catalysts showed the best SCR activity. However, for further applications, the temperature window at high NO conversion, N_2 selectivity, and stability of Mn-Ce composite oxides still need to be further improved. In addition, the catalytic mechanism of Ce-based catalysts is relatively complex and further research on this is required.

3.5. Cu-Based Catalyst

The Cu-based catalysts are widely applied in the NH_3-SCR reaction and feature Cu^{2+}/Cu^{+}, which is both an oxidation–reduction and acidic site [120]. Usually, an undoped CuO catalyst exhibits poor SCR catalytic performance compared with modified Cu-based catalysts. Yu et al. prepared a series of $CuO–V_2O_5/TiO_2$ catalysts for the SCR of NO with NH_3 and found that the addition of the Cu species promoted the production of more V^{4+} and chemisorbed oxygen in the V-Ti catalysts, resulting in enhanced NH_3-SCR catalytic performance [121]. Wang et al. [122] reported that the addition of copper in the V/Ti catalysts enhanced the number of acidic sites and active oxygen species on the catalyst and promoted good redox properties. Zheng et al. also studied the SCR performance of CuV/Ti catalysts and found that the NO conversion of the CuV/Ti catalysts reached 100% in the range of 220–330 °C with excellent N_2 selectivity. This is because the addition of CuO transformed the V/Ti catalyst from a single active center (V) to a dual active center (V + Cu) [123]. From this, it can be seen that CuO is a good additive for V-Ti catalytic systems. Moreover, Raja et al. [124] also reported TiO_2–carbon nanotube (CNT) loaded MnO_x–CuO catalysts for the NH_3-SCR of NO at low temperatures, and it was found that the addition of Cu improved the catalytic activity of the catalyst. Different Cu loadings had different effects on the SCR performance. The catalyst with 5 wt% Cu content was found to be the most active catalyst. Even in the presence of 200 ppm SO_2, the temperature window

for the Mn-Cu_5/Ti-CNTs for >90% NO conversion was still the widest at 200–300 °C, which was related to the increasing content of Mn^{4+} and chemical adsorption on the surface of the catalyst as a result of Cu loading. Researchers have also developed a new type of Mo-doped CuO catalyst for the low-temperature NH_3-SCR reaction. The NO_x conversion of a CuO catalyst doped with Mo was reported to be >80% at 175 °C. Mo doping into the CuO lattice forms Mo-O-Cu species, improving the adsorption of NH_3 and NO_x and promoting the formation of oxygen vacancies, which are important factors in promoting the SCR activity [125]. In addition, the sulfated Cu-based catalyst also exhibited excellent catalytic performance and sulfur resistance in the NH_3-SCR reaction.

A Cu-based catalyst surface sulfated by SO_2 forms new acidic sites, which inhibit the oxidation of NH_3 and enhance its resistance to SO_2. Yu et al. [126] prepared $CuSO_4/TiO_2$ catalysts with different $CuSO_4$ loading amounts (0–20 wt%). The effect of the copper(II) sulfate content on the catalytic activity was investigated. A high $CuSO_4$ loading was shown to be beneficial for the interaction between $CuSO_4$ and TiO_2. With an increase in $CuSO_4$ loading, the activity of the catalyst was significantly improved at <340 °C, however, the oxidation of NH_3 was also enhanced at >340 °C. A novel Cu-Ce-S catalyst was prepared by Shi et al. for the NH_3-SCR [127], where the S and Cu originated from $CuSO_4$. The NO_x conversion of the 3% Cu-Ce-S catalyst decreased by only 3% in the presence of H_2O and SO_2 due to the Cu^{2+} being doped into the CeO_2 lattice. During the reaction, SO_4^{2-} preferentially connected with Cu^{2+}, protecting the active site of Ce^{4+}. The $Cu^{2+} \leftrightarrow Cu^{+}$ and $Ce^{4+} \leftrightarrow Ce^{3+}$ redox cycles also enhanced the activity of the catalyst.

In addition to modifying Cu-based catalysts, special structures can also be designed to improve catalytic performance. Cu-based catalysts with a core–shell structure have been extensively studied for the SCR of NO_x by NH_3. Cu-based catalysts with a core–shell structure can achieve a dynamic equilibrium between NH_3 oxidation and NO_x reduction. Generated NO and NO_2 can diffuse from the core and react with NH_3 to form N_2, reducing the formation of the by-product N_2O. Yu et al. [128] designed and synthesized a CuO@Cu-MOF core-shell catalyst with CuO as the core and $Cu_3(BTC)_2$ as the shell via an in situ growth method for the NH_3-SCR reaction (Figure 9A). The CuO core in the catalyst exhibited excellent NO adsorption performance and reducibility, while the $Cu_3(BTC)_2$ shell also featured a large number of acidic sites. This material with abundant acidic sites and NO_x intermediate species promoted the low-temperature NH_3-SCR reaction. In addition, the CuO@Cu-MOF also showed satisfactory stability, making it a promising low-temperature SCR catalyst. In addition, the core–shell structure also prevented the low-temperature activity of the catalyst from being affected by SO_2 and water vapor. This new type of titanium dioxide-supported copper-doped phosphomolybdic acid (Cu-HPMo) was studied by Jiang et al. [129] As shown in Figure 9B, the Cu is the core and HPMo is the shell. The results show that when the Cu/Mo molar ratio is three, the Cu(3)-HPMo/TiO_2 catalyst shows the best SCR performance, with a denitrification efficiency of ≥99% at 200 °C, which does not decrease in the presence of 200 ppm SO_2 and 4×10^4 ppm H_2O. This indicates that strong acidity inhibits SO_2 adsorption and exhibits good resistance to SO_2. According to density functional theory calculation results, SO_2 is not chemisorbed on the HPMo surface, indicating that the catalyst with this structure exhibited the best sulfur resistance.

Based on the above research, modified Cu-based catalysts exhibit enhanced SCR catalytic performance. However, the operating temperature window for high NO conversion over Cu-based catalysts is relatively narrow, which is an important issue that needs to be resolved so that Cu-based oxide catalysts can be practically used. In addition, the low-temperature SCR activity of Cu-based oxide catalysts needs to be further improved.

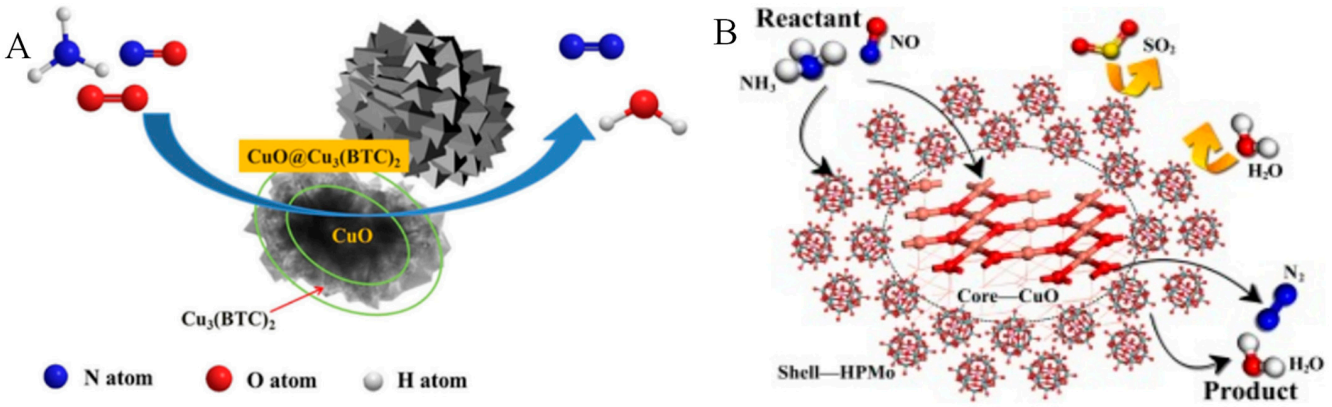

Figure 9. Schematic diagram of reaction mechanism of CuO@Cu-MOF (**A**) and Cu-HPMo (**B**) core-shell structure catalysts [128,129]. (**A**) Reprinted with permission from Ref. [128]. Copyright 2019, Wiley-VCH. (**B**) Reprinted with permission from Ref. [129]. Copyright 2020, Elsevier B.V.

4. The Stability of the SCR Catalyst

SCR devices are usually placed downstream of the diesel particulate filter (DPF), and therefore denitration catalysts need to be able to withstand the temperature of the DPF regeneration. Thus, it can be seen that improving the high-temperature stability of denitration catalysts is of great significance for diesel exhaust aftertreatment systems. The important factor that affects the high-temperature resistance of the catalyst is its surface acidity. Therefore, the high-temperature resistance of catalysts is generally enhanced by increasing their surface acidity. Acidic oxides, such as WO_3 and ZrO_2, are considered to be the optimal materials for improving high-temperature stability [130]. Chen et al. [131] prepared W-Zr-O_x/TiO_2 catalysts for the NH_3-SCR via a precipitation method. The loading of W-Zr-O_x resulted in having more acidic sites on the catalyst surface, better redox performance, and a higher proportion of oxygen vacancies, thereby improving the high-temperature activity of the catalyst. It has also been found that the interaction between WO_3 and ZrO_2 can improve the surface acidity and redox performance of a catalyst, which is beneficial to its excellent performance at high temperatures. Feng et al. [132] used different methods to prepare W-Zr-ZSM-5 catalysts, among which catalysts with rich acidic sites and excellent redox properties exhibited better deNO_x performance at high temperatures. In addition, cerium(IV) oxide, as an additive, formed a Ti-Ce-O_x catalyst with Ti and significantly improved the catalytic activity and thermal stability of the TiO_2 catalyst support. After high-temperature treatment for 24 h, the catalytic activity of Ti-Ce-O_x-500 remained unchanged at 400 °C. This excellent catalytic performance and stability were attributed to its high specific surface area, in addition to its abundant acidic sites and active oxygen species. In addition, cerium atoms have been shown to prevent grain growth and protect the pore structure of catalysts at high temperatures [133].

However, when a diesel engine is cold started or operated under low engine load, there are also requirements for the low-temperature catalytic performance of denitration catalysts. Currently, the low-temperature activity of denitration catalysts is usually improved by adding metal oxides. Among them, Mn-based catalysts exhibit high low-temperature activity due to their variable valence states and excellent redox properties. However, the operating temperature window for high NO conversion over MnO_x is relatively narrow and the water- and sulfur-resistant performance needs to be improved (see Section 3.2 for details).

5. Conclusions and Outlook

NO_x, as one of the main pollutants in diesel vehicle exhaust, seriously endangers the atmospheric environment and human health. Therefore, the elimination of NO_x has become the focus of research. At present, the most effective and widely used technology for controlling NO_x from diesel vehicle exhaust is NH_3-SCR technology. This paper introduced

the reactions that existed in the NH_3-SCR reaction process and their relationships. And the research progress of metal oxide catalysts for the NH_3-SCR reaction was also described, mainly including V-based catalysts, Mn-based catalysts, Fe-based catalysts, Ce-based catalysts, and Cu-based catalysts. V-based catalysts as mature commercial catalysts were studied earlier. Mn-based catalysts have the best low-temperature SCR performance. The Fe-based catalysts, Ce-based catalysts and Cu-based catalysts with good catalytic performance have also attracted attention. However, there are still many problems and challenges in the application of metal oxide catalysts for NO_x control, and further research is needed. Therefore, the following issues need to be addressed in future research on metal oxide catalysts:

(1) The metal oxide catalysts have disadvantages, such as narrow operating temperature windows basically within the low or medium–low temperature range and poor N_2 selectivity. Therefore, modifying catalysts to enhance their NH_3-SCR catalytic performance is the main focus of future research.
(2) The presence of H_2O and SO_2 are definite in diesel vehicle exhaust and metal oxides can easily react with them to deactivate the catalyst, therefore, improving the hydrothermal stability and SO_2 tolerance of the catalyst remains the major factor of the SCR technology.
(3) Further research needs to be focused on the reaction mechanisms of sulfur dioxide and water poisoning processes for catalysts. The studies of catalyst poisoning mechanisms cannot determine the process of catalyst poisoning only through in situ characterization technology. The synchrotron-radiation, theoretical calculations, and isotopic tracer techniques should also be considered to fully explain the mechanisms of the catalyst poisoning process.
(4) The injection of NH_3 is a major component of the SCR device, but there may be blockages in the NH_3 injection on occasion and the NH_3 amount is imprecise. Therefore, optimizing the injection way and accurately controlling the injection amount will be one of the important goals.

Author Contributions: Literature search, L.W., S.Z. and C.Z.; article structure design, X.Y. and Z.Z.; manuscript writing, L.W.; graphics production, M.Y.; creating diagrams, D.Y. and S.G.; manuscript revision, L.W. and X.Y. All authors have read and agreed to the published version of the manuscript.

Funding: This work was financially supported by the National Key R&D Program of China (2022YFB3506200, 2022YFB3504100); National Natural Science Foundation of China (22072095, U1908204); Liaoning Provincial Central Government Guides Local Science and Technology Development Funds (2022JH6/100100052); Excellent Youth Science Foundation of Liaoning Province (2022-YQ-20); Shenyang Science and Technology Planning Project (22-322-3-28); University Joint Education Project for China-Central and Eastern European Countries (2021097); Major/Key Project of Graduate Education and Teaching Reform of Shenyang Normal University (YJSJG120210008/YJSJG220210022); University level innovation team of Shenyang Normal University.

Data Availability Statement: Not applicable.

Conflicts of Interest: The authors declare no conflict of interest.

References

1. Jiaqiang, E.; Liu, G.; Zhang, Z.; Han, D.; Chen, J.; Wei, K.; Gong, J.; Yin, Z. Effect analysis on cold starting performance enhancement of a diesel engine fueled with biodiesel fuel based on an improved thermodynamic model. *Appl. Energy* **2019**, *243*, 321–335. [CrossRef]
2. Cai, T.; Zhao, D.; Wang, B.; Li, J.W.; Guan, Y.H. NO_x emission and thermal performances studies on premixed ammonia-oxygen combustion in a CO_2-free micro-planar combustor. *Fuel* **2020**, *280*, 118554. [CrossRef]
3. Zhang, Z.; Jiaqiang, E.; Chen, J.; Zhao, X.; Zhang, B.; Deng, Y.; Peng, Q.; Yin, Z. Effects of boiling heat transfer on the performance enhancement of a medium speed diesel engine fueled with diesel and rapeseed methyl ester. *Appl. Therm. Eng.* **2020**, *169*, 114984. [CrossRef]
4. Balasubramanian, R.; Gao, X.; Hatakeyama, S.; Hwang, J.; Tsai, C.J. Overview of the Special Issue "PM2.5 in Asia" for 2015 Asian Aerosol Conference. *Aerosol Air Qual. Res.* **2017**, *17*, 351–355. [CrossRef]

5. Hadidi, L.A.; Aldosary, A.S.; Al-Matar, A.K.; Mudallah, O.A. An optimization model to improve gas emission mitigation in oil refineries. *J. Clean. Prod.* **2016**, *118*, 29–36. [CrossRef]
6. Chen, R.; Zhang, T.S.; Guo, Y.Q.; Wang, J.W.; Wei, J.X.; Yu, Q.J. Recent advances in simultaneous removal of SO_2 and NO_x from exhaust gases: Removal process, mechanism and kinetics. *Chem. Eng. J.* **2021**, *420*, 127588. [CrossRef]
7. Balayeva, N.O.; Mamiyev, Z. Chapter 5—Integrated processes involving adsorption, photolysis, and photocatalysis. In *Hybrid and Combined Processes for Air Pollution Control*; Elsevier: Amsterdam, The Netherlands, 2022; pp. 117–153.
8. Khanal, V.; Balayeva, N.O.; Günnemann, C.G.; Mamiyev, Z.; Dillert, R.; Bahnemann, D.W.; Subramanian, V. Photocatalytic NO_x removal using tantalum oxide nanoparticles: A benign pathway. *Appl. Catal. B Environ.* **2021**, *291*, 119974. [CrossRef]
9. Wang, L.Y.; Ren, Y.; Yu, X.H.; Peng, C.; Yu, D.; Zhong, C.M.; Hou, J.; Yin, C.Y.; Fan, X.Q.; Zhao, Z.; et al. Novel preparation method, catalytic performance and reaction mechanisms of $Pr_xMn_{1-x}O_\delta$/3DOM ZSM-5 catalysts for the simultaneous removal of soot and NO_x. *J. Catal.* **2023**, *417*, 226–247. [CrossRef]
10. Liu, Y.X.; Wang, Q.; Pan, J.F. Novel process on simultaneous removal of nitric oxide and sulfur dioxide using vacuum ultraviolet (VUV)-activated $O_2/H_2O/H_2O_2$ system in a wet VUV-spraying reactor. *Environ. Sci. Technol.* **2016**, *50*, 12966–12975. [CrossRef] [PubMed]
11. Asghar, U.; Rafiq, S.; Anwar, A.; Iqbal, T.; Ahmed, A.; Jamil, F.; Khurram, M.S.; Akbar, G.; Farooq, A.; Shah, N.S.; et al. Review on the progress in emission control technologies for the abatement of CO_2, SO_x and NO_x from fuel combustion. *J. Environ. Chem. Eng.* **2021**, *9*, 106064. [CrossRef]
12. Pan, Y.R.; Zhang, Y.; Zhou, T.T.; Louis, B.; O'Hare, D.; Wang, Q. Fabrication of lithium silicates as highly efficient high-temperature CO_2 sorbents from SBA-15 precursor. *Inorg. Chem.* **2017**, *56*, 7821–7834. [CrossRef] [PubMed]
13. Li, W.J.; Li, T.Y.; Wey, M.Y. Preferred enhancement of fast-SCR by Mn/$CeSiO_x$ catalyst: Study on Ce/Si promotion and shape dependence. *Chem. Eng. J.* **2021**, *403*, 126317. [CrossRef]
14. Wang, L.Y.; Yu, X.H.; Wei, Y.C.; Liu, J.; Zhao, Z. Research advances of rare earth catalysts for catalytic purification of vehicle exhausts. *J. Rare Earths* **2021**, *39*, 1151–1180. [CrossRef]
15. Boningari, T.; Pappas, D.K.; Smirniotis, P.G. Metal oxide-confined interweaved titania nanotubes M/TNT (M = Mn, Cu, Ce, Fe, V, Cr, and Co) for the selective catalytic reduction of NO_x in the presence of excess oxygen. *J. Catal.* **2018**, *365*, 320–333. [CrossRef]
16. Han, L.P.; Cai, S.X.; Gao, M.; Hasegawa, J.Y.; Wang, P.L.; Zhang, J.P.; Shi, L.Y.; Zhang, D.S. Selective catalytic reduction of NO_x with NH_3 by using novel catalysts: State of the art and future prospects. *Chem. Rev.* **2019**, *119*, 10916–10976. [CrossRef]
17. Byun, S.W.; Lee, S.J.; Kim, M.; Bae, W.B.; Shin, H.; Hazlett, M.J.; Kang, D.; Tesfaye, B.; Park, P.W.; Kang, S.B. High N_2 selectivity of Pt-V-W/TiO_2 oxidation catalyst for simultaneous control of NH_3 and CO emissions. *Chem. Eng. J.* **2022**, *444*, 136517. [CrossRef]
18. Wang, W.; Herreros, J.M.; Tsolakis, A.; York, A.P.E. Increased NO_2 concentration in the diesel engine exhaust for improved Ag/Al_2O_3 catalyst NH_3-SCR activity. *Chem. Eng. J.* **2015**, *270*, 582–589. [CrossRef]
19. Gillot, S.; Tricot, G.; Vezin, H.; Dacquin, J.P.; Dujardin, C.; Granger, P. Induced effect of tungsten incorporation on the catalytic properties of $CeVO_4$ systems for the selective reduction of NO_x by ammonia. *Appl. Catal. B* **2018**, *234*, 318–328. [CrossRef]
20. Mu, J.; Li, X.; Sun, W.; Fan, S.; Wang, X.; Wang, L.; Qin, M.; Gan, G.; Yin, Z.; Zhang, D. Inductive effect boosting catalytic performance of advanced $Fe_{1-x}V_xO_\delta$ catalysts in Low-temperature NH_3 selective catalytic reduction: Insight into the structure, interaction, and mechanisms. *ACS Catal.* **2018**, *8*, 6760–6774. [CrossRef]
21. Wang, Y.; Ji, X.; Meng, H.; Qu, L.; Wu, X. Fabrication of high-silica Cu/ZSM-5 with confinement encapsulated Cu-based active species for NH_3-SCR. *Catal. Commun.* **2020**, *138*, 105969. [CrossRef]
22. Perumal, S.K.; Kaisare, N.; Kummari, S.K.; Aghalayam, P. Low-temperature NH_3-SCR of NO over robust RuNi/Al-SBA-15 catalysts: Effect of Ru loading. *J. Environ. Chem. Eng.* **2022**, *10*, 108288. [CrossRef]
23. Wang, H.J.; Huang, B.C.; Yu, C.L.; Lu, M.J.; Huang, H.; Zhou, Y.L. Research progress, challenges and perspectives on the sulfur and water resistance of catalysts for low temperature selective catalytic reduction of NO_x by NH_3. *Appl. Catal. A* **2019**, *588*, 117207. [CrossRef]
24. Sun, Y.; Fu, Y.; Shan, Y.L.; Du, J.P.; Liu, Z.Q.; Gao, M.; Shi, X.Y.; He, G.Z.; Xue, S.; Han, X.W.; et al. Si/Al ratio determines the SCR performance of Cu-SSZ-13 catalysts in the presence of NO_2. *Environ. Sci. Technol.* **2022**, *56*, 17946–17954. [CrossRef] [PubMed]
25. Bendrich, M.; Scheuer, A.; Hayes, R.E.; Votsmeier, M. Unified mechanistic model for standard SCR, fast SCR, and NO_2-SCR over a copper chabazite catalyst. *Appl. Catal. B* **2018**, *222*, 76–87. [CrossRef]
26. Andana, T.; Rapp'e, K.J.; Ga, F.; Szanyi, J.; Pereira-Hernandez, X.; Wang, Y. Recent advances in hybrid metal oxide–zeolite catalysts for low-temperature selective catalytic reduction of NO_x by ammonia. *Appl. Catal. B* **2021**, *291*, 120054. [CrossRef]
27. Liu, K.; He, H.; Chu, B.W. Microkinetic study of NO oxidation, standard and fast NH_3-SCR on $CeWO_x$ at low temperatures. *Chem. Eng. J.* **2021**, *423*, 130128. [CrossRef]
28. Janssens, T.V.W.; Falsig, H.; Lundegaard, L.F.; Vennestrøm, P.N.R.; Rasmussen, S.B.; Moses, P.G.; Giordanino, F.; Borfecchia, E.; Lomachenko, K.A.; Lamberti, C.; et al. A consistent reaction scheme for the selective catalytic reduction of nitrogen oxides with ammonia. *ACS Catal.* **2015**, *5*, 2832–2845. [CrossRef]
29. Shi, Z.; Peng, Q.; Jiaqiang, E.; Xie, B.; Wei, J.; Yin, R.; Fu, G. Mechanism, performance and modification methods for NH_3-SCR catalysts: A review. *Fuel* **2023**, *331*, 125885. [CrossRef]
30. Ye, D.; Qu, R.; Song, H.; Gao, X.; Luo, Z.; Ni, M.; Cen, K. New Insights into the Various Decomposition and Reactivity Behaviors of NH_4HSO_4 with NO on V_2O_5/TiO_2 Catalyst Surfaces. *Chem. Eng. J.* **2016**, *283*, 846–854. [CrossRef]

31. Zheng, W.; Chen, J.L.; Guo, L.; Zhang, W.B.; Zhao, H.R.; Wu, X.Q. Research progress of hydrothermal stability of metal-based zeolite catalysts in NH_3-SCR reaction. *J. Fuel Chem. Technol.* **2020**, *48*, 1193–1207. [CrossRef]
32. Xie, R.Y.; Ma, L.; Li, Z.H.; Qu, Z.; Yan, N.Q.; Li, J.H. Review of sulfur promotion effects on metal oxide catalysts for NO_x emission control. *ACS Catal.* **2021**, *11*, 13119–13139. [CrossRef]
33. Xu, T.F.; Wu, X.D.; Gao, Y.X.; Lin, Q.W.; Hu, J.F.; Weng, D. Comparative study on sulfur poisoning of V_2O_5-Sb_2O_3/TiO_2 and V_2O_5-WO_3/TiO_2 monolithic catalysts for low-temperature NH_3-SCR. *Catal. Commun.* **2017**, *93*, 33–36. [CrossRef]
34. Wang, B.; Bian, Y.; Feng, S.; Wang, S.Q.; Shen, B.X. Modification of the V_2O_5-WO_3/TiO_2 catalyst with Nb to reduce its activity for SO_2 oxidation during the selective catalytic reduction of NO_x. *J. Fuel Chem. Technol.* **2022**, *50*, 503–512. [CrossRef]
35. Jung, Y.J.; Cha, J.S.; Kim, B.S. Characteristics of deactivation and thermal regeneration of Nb-doped V_2O_5–WO_3/TiO_2 catalyst for NH_3–SCR reaction. *Environ. Res.* **2023**, *227*, 115744. [CrossRef] [PubMed]
36. Shi, A.; Wang, X.; Yu, T.; Shen, M. The Effect of Zirconia additive on the activity and structure stability of V_2O_5/WO_3-TiO_2 ammonia SCR catalysts. *Appl. Catal. B* **2011**, *106*, 359–369. [CrossRef]
37. Kang, T.H.; Youn, S.; Kim, D.H. Improved catalytic performance and resistance to SO_2 over V_2O_5-WO_3/TiO_2 catalyst physically mixed with Fe_2O_3 for low-temperature NH_3-SCR. *Catal. Today* **2021**, *376*, 95–103. [CrossRef]
38. Jeon, S.W.; Song, I.; Lee, H.; Kim, J.; Byun, Y.; Koh, D.J.; Kim, D.H. Enhanced SO_2 resistance of V_2O_5/WO_3-TiO_2 catalyst physically mixed with alumina for the selective catalytic reduction of NO_x with NH_3. *Chem. Eng. J.* **2022**, *433*, 133836. [CrossRef]
39. Ni, K.W.; Peng, Y.W.; Dai, G.Y.; Zhao, H.W.; Huang, Z.W.; Wu, X.M.; Jing, G.H.; Feng, W.; Yuan, Y. Ceria accelerates ammonium bisulfate decomposition for improved SO_2 resistance on a V_2O_5-WO_3/TiO_2 catalyst in low-temperature NH_3-SCR. *J. Taiwan Inst. Chem. Eng.* **2022**, *140*, 104555. [CrossRef]
40. Song, L.; Chao, J.; Fang, Y.; He, H.; Li, J.; Qiu, W.; Zhang, G. Promotion of ceria for decomposition of ammonia bisulfate over V_2O_5-MoO_3/TiO_2 catalyst for selective catalytic reduction. *Chem. Eng. J.* **2016**, *303*, 275–281. [CrossRef]
41. Wang, Y.; Yi, W.; Yu, J.; Zeng, J.; Chang, H. Novel methods for assessing the SO_2 poisoning effect and thermal regeneration possibility of MO_x-WO_3/TiO_2 (M = Fe, Mn, Cu, and V) catalysts for NH_3-SCR. *Environ. Sci. Technol.* **2020**, *54*, 12612–12620. [CrossRef]
42. Lee, K.J.; Kumar, P.A.; Maqbool, M.S.; Rao, K.N.; Song, K.H.; Ha, H.P. Ceria added Sb-V_2O_5/TiO_2 catalysts for low-temperature NH_3-SCR: Physico-Chemical properties and catalytic activity. *Appl. Catal. B* **2013**, *142–143*, 705–717. [CrossRef]
43. Cao, J.; Yao, X.; Yang, F.; Chen, L.; Fu, M.; Tang, C.; Dong, L. Improving the deNO_x performance and K-poisoning resistance of the V_2O_5-WO_3/TiO_2 catalyst by Ce^{4+} and Zr^{4+} co-doping. *Chin. J. Catal.* **2019**, *40*, 95–104. [CrossRef]
44. Wang, H.Y.; Wang, B.D.; Sun, Q.; Li, Y.L.; Xu, W.Q.; Li, J.H. New insights into the promotional effects of Cu and Fe over V_2O_5-WO_3/TiO_2 NH_3-SCR catalysts towards oxidation of Hg0. *Catal. Commun.* **2017**, *100*, 169–172. [CrossRef]
45. Liu, X.; Wu, X.; Xu, T.; Weng, D.; Si, Z.; Ran, R. Effects of silica additive on the NH_3-SCR activity and thermal stability of a V_2O_5/WO_3-TiO_2 catalyst. *Chin. J. Catal.* **2016**, *37*, 1340–1346. [CrossRef]
46. Shao, X.Z.; Wang, H.Y.; Yuan, M.L.; Yang, J.; Zhan, W.C.; Wang, L.; Guo, Y.; Lu, G.Z. Thermal stability of Si-doped V_2O_5/WO_3–TiO_2 for selective catalytic reduction of NO_x by NH_3. *Rare Metals* **2019**, *38*, 292–298. [CrossRef]
47. Ren, S.; Yang, J.; Zhang, T.S.; Jiang, L.J.; Long, H.M.; Guo, F.Q.; Kong, M. Role of cerium in improving NO reduction with NH_3 over Mn-Ce/ASC catalyst in low-temperature flue gas. *Chem. Eng. Res. Des.* **2018**, *133*, 1–10. [CrossRef]
48. Yang, J.; Ren, S.; Zhou, Y.H.; Su, Z.H.; Yao, L.; Cao, J.; Jiang, L.J.; Hu, J.; Kong, M.; Yang, J.; et al. In situ IR comparative study on N_2O formation pathways over different valence states manganese oxides catalysts during NH_3–SCR of NO. *Chem. Eng. J.* **2020**, *397*, 125446. [CrossRef]
49. Thirupathi, B.; Smirniotis, P.G. Nickel-doped Mn/TiO_2 as an efficient catalyst for the low-temperature SCR of NO with NH_3: Catalytic evaluation and characterizations. *J. Catal.* **2012**, *288*, 74–83. [CrossRef]
50. Yang, J.; Ren, S.; Su, B.; Zhou, Y.; Hu, G.; Jiang, L.; Cao, J.; Liu, W.; Yao, L.; Kong, M.; et al. Insight into N_2O formation over different crystal phases of MnO_2 during low-temperature NH_3-SCR of NO. *Catal. Lett.* **2021**, *151*, 2964–2971. [CrossRef]
51. Liang, Y.J.; Gao, C.; Zhang, Z.R.; Wang, B.; Xuan, Y.; Tong, K.B.; Wang, Y.Z.; Yun, Y.; Wang, D.; Peng, Y. Modulation of paired acid centers for the α-, β-, γ- and δ-MnO_2 for the NH_3-SCR: A comparative density functional theory (DFT) study. *Mol. Catal.* **2023**, *546*, 113252. [CrossRef]
52. Fang, D.; Xie, J.L.; Hu, H.; Yang, H.; He, F.; Fu, Z.B. Identification of MnO_x species and Mn valence states in MnO_x/TiO_2 catalysts for low temperature SCR. *Chem. Eng. J.* **2015**, *271*, 23–30. [CrossRef]
53. He, G.Z.; Gao, M.; Peng, Y.; Yu, Y.B.; Shan, W.P.; He, H. Superior oxidative dehydrogenation performance toward NH_3 determines the excellent low-temperature NH_3 -SCR activity of Mn-based catalysts. *Environ. Sci. Technol.* **2021**, *55*, 6995–7003. [CrossRef] [PubMed]
54. Jiang, H.X.; Wang, J.; Zhou, J.L.; Chen, Y.F.; Zhang, M.H. Effect of promoters on the catalytic performance and SO_2/H_2O resistance of α-MnO_2 catalysts for low temperature NH_3-SCR. *Ind. Eng. Chem. Res.* **2019**, *58*, 1760–1768. [CrossRef]
55. Dong, Y.; Jin, B.; Liu, S.; Gao, J.; Wang, K.; Su, F. Abundant oxygen vacancies induced by the mechanochemical process boost the low-temperature catalytic performance of MnO_2 in NH_3-SCR. *Catalysts* **2022**, *12*, 1291. [CrossRef]
56. Zhan, S.H.; Zhu, D.D.; Qiu, M.Y.; Yu, H.B.; Li, Y. Highly efficient removal of NO with ordered mesoporous manganese oxide at low temperature. *RSC Adv.* **2015**, *5*, 29353–29361. [CrossRef]

57. Liu, J.; Wei, Y.J.; Li, P.Z.; Zhang, P.P.; Su, W.; Sun, Y.; Zou, R.Q.; Zhao, Y.L. Experimental and theoretical investigation of mesoporous MnO_2 nanosheets with oxygen vacancies for high-efficiency catalytic deNO_x. *ACS Catal.* **2018**, *8*, 3865–3874. [CrossRef]
58. Liu, F.Y.; Li, J.Q.; Chen, C.Y.; Ning, D.Y.; Yang, J.; Chu, Z.Y.; Mao, X.S.; Lan, Y.P. Low-temperature NO_x selective catalytic reduction activity evaluation of hollow-spherical manganese oxides. *Res. Chem. Intermediat.* **2022**, *48*, 3007–3018. [CrossRef]
59. Geng, Y.; Shan, W.; Liu, F.; Yang, S. Adjustment of operation temperature window of Mn-Ce oxide catalyst for the selective catalytic reduction of NO_x with NH_3. *J. Hazard. Mater.* **2021**, *405*, 124223. [CrossRef]
60. Li, Y.F.; Hou, Y.Q.; Zhang, Y.Z.; Yang, Y.T.; Huang, Z.G. Confinement of MnO_x@Fe_2O_3 core-shell catalyst with titania nanotubes: Enhanced N_2 selectivity and SO_2 tolerance in NH_3- SCR process. *J. Colloid Interf. Sci.* **2022**, *608*, 2224–2234. [CrossRef]
61. Chen, Z.; Yang, Q.; Li, H.; Li, X.; Wang, L.; Chi, T.S. Cr–MnO_x mixed-oxide catalysts for selective catalytic reduction of NO_x with NH_3 at low temperature. *J. Catal.* **2010**, *276*, 56–65. [CrossRef]
62. Chen, W.B.; Zou, R.Q.; Wang, X.D. Toward an atomic-level understanding of the catalytic mechanism of selective catalytic reduction of NO_x with NH_3. *ACS Catal.* **2022**, *12*, 14347–14375. [CrossRef]
63. Jin, R.B.; Liu, Y.; Wang, Y.; Cen, W.L.; Wu, Z.B.; Wang, H.Q.; Weng, X.L. The role of cerium in the improved SO_2 tolerance for NO reduction with NH_3 over Mn-Ce/TiO_2 catalyst at low temperature. *Appl. Catal. B* **2014**, *148–149*, 582–588. [CrossRef]
64. Yang, W.W.; Gong, J.; Wang, X.; Bao, Z.H.; Guo, Y.B.; Wu, Z.L. A Review on the impact of SO_2 on the oxidation of NO, hydrocarbons, and CO in diesel emission control catalysis. *ACS Catal.* **2021**, *11*, 12446–12468. [CrossRef]
65. Wang, Z.H.; Chen, B.B.; Zhao, Q.; Crocker, M.; Li, Y.J.; Shi, C. Metal-support interaction induced atomic dispersion and redispersion of Pd on CeO_2 for passive NO_x adsorption. *Chem. Eng. J.* **2023**, *11*, 144080. [CrossRef]
66. Chen, L.; Ren, S.; Xing, X.D.; Yang, J.; Jiang, L.; Yang, J.; Liu, Q.C. Effect of MnO_2 crystal types on CeO_2@MnO_2 oxides catalysts for low-temperature NH_3-SCR. *J. Environ. Chem. Eng.* **2022**, *10*, 108239. [CrossRef]
67. Wang, M.M.; Ren, S.; Xing, X.D.; Zhou, Y.H.; Yang, J.; Chen, L.; Li, X.D. Catalytic performance of CeO_2-NPs and α-MnO_2 mixed oxides catalysts for low-temperature NH_3-SCR of NO. *J. Energy Inst.* **2022**, *103*, 54–59. [CrossRef]
68. Qin, Q.J.; Chen, K.A.; Xie, S.Z.; Li, L.L.; Ou, X.M.; Wei, X.L.; Luo, X.T.; Dong, L.H.; Li, B. Enhanced SO_2 and H_2O resistance of $MnTiSnO_y$ composite oxide for NH_3-SCR through Sm modification. *Appl. Surf. Sci.* **2022**, *583*, 152478. [CrossRef]
69. Meng, D.M.; Zhan, W.C.; Guo, Y.; Guo, Y.L.; Wang, L.; Lu, G.Z. A highly effective catalyst of Sm-MnO_x for the NH_3-SCR of NO_x at low temperature: Promotional role of Sm and its catalytic performance. *ACS Catal.* **2015**, *5*, 5973–5983. [CrossRef]
70. Chen, Z.C.; Ren, S.; Wang, M.M.; Yang, J.; Chen, L.; Liu, W.Z.; Liu, Q.C.; Su, B.X. Insights into samarium doping effects on catalytic activity and SO_2 tolerance of $MnFeO_x$ catalyst for low-temperature NH_3-SCR reaction. *Fuel* **2022**, *321*, 124113. [CrossRef]
71. Li, H.X.; Jin, L.Y.; Zhang, A.C.; Sun, Z.J.; Zhang, X.M.; Zhu, Q.F.; Yang, C.Z.; Zhang, S.B. Investigation of Co-doped Mn oxide catalyst for NH_3-SCR activity and SO_2/H_2O resistance. *J. Fuel Chem. Technol.* **2022**, *50*, 1404–1416. [CrossRef]
72. Wan, Y.P.; Zhao, W.R.; Tang, Y.; Li, L.; Wang, H.J.; Cui, Y.L.; Gu, J.L.; Li, Y.S.; Shi, J.L. Ni-Mn bi-metal oxide catalysts for the low temperature SCR removal of NO with NH_3. *Appl. Catal. B* **2014**, *148–149*, 114–122. [CrossRef]
73. Shi, Y.R.; Yi, H.H.; Gao, F.Y.; Zhao, S.Z.; Xie, Z.L.; Tang, X.L. Evolution mechanism of transition metal in NH_3-SCR reaction over Mn-based bimetallic oxide catalysts: Structure-activity relationships. *J. Hazard. Mater.* **2021**, *413*, 125361. [CrossRef] [PubMed]
74. Zhang, W.S.; Shi, X.Y.; Yan, Z.D.; Shan, Y.L.; Zhu, Y.; Yu, Y.B.; He, H. Design of high-performance iron–niobium composite oxide catalysts for NH_3-SCR: Insights into the interaction between Fe and Nb. *ACS Catal.* **2021**, *11*, 9825–9836. [CrossRef]
75. Shi, J.; Zhang, Y.; Zhu, Y.; Chen, M.X.; Zhang, Z.X.; Shangguan, W.F. Efficient Fe-ZSM-5 catalyst with wide active temperature window for NH_3 selective catalytic reduction of NO: Synergistic effect of isolated Fe^{3+} and Fe_2O_3. *J. Catal.* **2019**, *378*, 17–27. [CrossRef]
76. Jian, Y.F.; Yu, T.T.; Jiang, Z.Y.; Yu, Y.K.; Douthwaite, M.; Liu, J.Y.; Albilali, R.; He, C. In-depth understanding of the morphology effect of a-Fe_2O_3 on catalytic ethane destruction. *ACS Appl. Mater. Interfaces* **2019**, *11*, 11369. [CrossRef]
77. Zhou, Z.Z.; Li, W.H.; Liu, Z.M. Significantly enhanced catalytic performance of $Fe_2(SO_4)_3/CeO_2$ catalyst for the selective catalytic reduction of NO_x by NH_3. *Ind. Eng. Chem. Res.* **2021**, *60*, 15472–15478. [CrossRef]
78. Yu, Y.; Chen, C.; Ma, M.; Douthwaite, M.; He, C.; Miao, J.; Chen, J.; Li, C. SO_2 Promoted in situ recovery of thermally deactivated $Fe_2(SO_4)_3/TiO_2$ NH_3-SCR catalysts: From experimental work to theoretical study. *Chem. Eng. J.* **2019**, *361*, 820–829. [CrossRef]
79. Ni, J.; Peng, X.B.; Yang, L.L.; Zhang, K.; Zhang, Y.Y.; Zhou, Y.L.; Wang, X.Y.; Au, C.T.; Jiang, L.L. Effects of cerium and tungsten addition on acid–base properties of spindle-like α-Fe_2O_3 in low-temperature SCR of NO_x with NH_3. *J. Rare Earth.* **2022**, *40*, 1734–1742. [CrossRef]
80. Chen, W.; Yang, S.; Liu, H.; Huang, F.; Shao, Q.H.; Liu, L.; Sun, J.; Sun, C.; Chen, D.; Dong, L. Single-atom Ce-modified α-Fe_2O_3 for selective catalytic reduction of NO with NH_3. *Environ. Sci. Technol.* **2022**, *56*, 10442–10453. [CrossRef]
81. Husnain, N.; Wang, E.; Fareed, S.; Anwar, M.T. Comparision on the low-temperature NH_3-SCR performance of γ-Fe_2O_3 catalysts prepared by two ddifferent methods. *Catalysts* **2019**, *9*, 1018. [CrossRef]
82. Mou, X.; Zhang, B.; Li, Y.; Yao, L.; Wei, X.; Su, D.S.; Shen, W. Rod-shaped Fe_2O_3 as an efficient catalyst for the selective reduction of nitrogen oxide by ammonia. *Angew. Chem. Int. Ed.* **2012**, *51*, 2989–2993. [CrossRef]
83. Yu, Y.; Tan, W.; An, D.; Wang, X.; Liu, A.; Zou, W.; Tang, C.; Ge, C.; Tong, Q.; Sun, J.; et al. Insight into the SO_2 resistance mechanism on γ-Fe_2O_3 catalyst in NH_3-SCR reaction: A collaborated experimental and DFT study. *Appl. Catal. B* **2021**, *281*, 119544. [CrossRef]

84. Sun, J.F.; Lu, Y.Y.; Zhang, L.; Ge, C.Y.; Tang, C.J.; Wan, H.Q.; Dong, L. Comparative study of different doped metal cations on the reduction, acidity, and activity of $Fe_9M_1O_x$ (M = Ti^{4+}, $Ce^{4+/3+}$, Al^{3+}) catalysts for NH_3-SCR reaction. *Ind. Eng. Chem. Res.* **2017**, *56*, 12101–12110. [CrossRef]
85. Fan, Y.X.; Zhang, J.; Yang, L.X.; Lu, M.X.; Ying, T.T.; Deng, B.H.; Dai, W.L.; Luo, X.B.; Zou, J.P.; Luo, S.L. Enhancing SO_2-shielding effect and Lewis acid sites for high efficiency in low-temperature SCR of NO with NH_3: Reinforced electron-deficient extent of Fe^{3+} enabled by Ti^{4+} in Fe_2O_3. *Sep. Purif. Technol.* **2023**, *311*, 123272. [CrossRef]
86. Sun, C.Z.; Chen, W.; Jia, X.X.; Liu, A.N.; Gao, F.; Feng, S.; Dong, L. Comprehensive understanding of the superior performance of Sm-modified Fe_2O_3 catalysts with regard to NO conversion and H_2O/SO_2 resistance in the NH_3-SCR reaction. *Chin. J. Catal.* **2021**, *42*, 417–430. [CrossRef]
87. Zhang, Y.K.; Xion, Z.B.; Yang, Q.G.; Zhou, F.; Lu, W.; Shi, H.C. Influence of copper doping on the low-medium NH_3-SCR activity of magnetic W/Fe_2O_3 catalyst: Its synergetic effect of glucose dosage. *J. Environ. Chem. Eng.* **2022**, *10*, 108694. [CrossRef]
88. Fan, H.; Wang, R. Low-temperature NH_3-SCR reaction over 3D Cu/Fe-TiO_2-rGO composite catalyst synthesized by photoreduction method. *Chem. Eng. J.* **2022**, *450*, 138152. [CrossRef]
89. Liu, Z.M.; Su, H.; Chen, B.H.; Li, J.H.; Woo, S.I. Activity enhancement of WO_3 modified Fe_2O_3 catalyst for the selective catalytic reduction of NO_x by NH_3. *Chem. Eng. J.* **2016**, *299*, 255–262. [CrossRef]
90. Wang, H.M.; Ning, P.; Zhang, Y.Q.; Ma, Y.P.; Wang, J.F.; Wang, L.Y.; Zhang, Q.L. Highly efficient WO_3-FeO_x catalysts synthesized using a novel solvent-free method for NH_3-SCR. *J. Hazard. Mater.* **2020**, *388*, 121812. [CrossRef]
91. Kang, L.; Han, L.P.; He, J.B.; Li, H.R.; Yan, T.T.; Chen, G.R.; Zhang, J.P.; Shi, L.Y.; Zhang, D.S. Improved NO_x reduction in the presence of SO_2 by using Fe_2O_3-promoted halloysite-supported CeO_2–WO_3 catalysts. *Environ. Sci. Technol.* **2019**, *53*, 938–945. [CrossRef] [PubMed]
92. Lian, Z.H.; Shan, W.P.; Zhang, Y.; Wang, M.; He, H. Morphology-Dependent catalytic performance of NbO_x/CeO_2 catalysts for selective catalytic reduction of NO_x with NH_3. *Ind. Eng. Chem. Res.* **2018**, *57*, 12736–12741. [CrossRef]
93. Zhang, B.L.; Zhang, S.G.; Liu, B. Effect of oxygen vacancies on ceria catalyst for selective catalytic reduction of NO with NH_3. *Appl. Surf. Sci.* **2020**, *529*, 147068. [CrossRef]
94. Chen, Y.F.; Zhang, Y.C.; Feng, X.; Li, J.L.; Liu, W.Z.; Ren, S.; Yang, J.; Liu, Q.C. In situ deposition of 0D CeO_2 quantum dots on Fe_2O_3-containing solid waste NH_3-SCR catalyst: Enhancing redox and NH_3 adsorption ability. *Waste Manage.* **2022**, *149*, 323–332. [CrossRef] [PubMed]
95. Zhou, Y.H.; Ren, S.; Rang, J.; Liu, W.Z.; Su, Z.H.; Chen, Z.C.; Wang, M.M.; Chen, L. NH_3 treatment of CeO_2 nanorods catalyst for improving NH_3-SCR of NO. *J. Energy Inst.* **2021**, *98*, 199–205. [CrossRef]
96. Ma, L.; Seo, C.Y.; Nahata, M.; Chen, X.Y.; Li, J.H.; Schwank, J.W. Shape dependence and sulfate promotion of CeO_2 for selective catalytic reduction of NO with NH_3. *Appl. Catal. B* **2018**, *232*, 246–259. [CrossRef]
97. Le, M.T.; Singh, S.; Quang, M.N.; Ngo, A.B.; Brückner, A.; Armbruster, U. Insight into the properties of MnO_2-Co_3O_4-CeO_2 catalyst series for the selective catalytic reduction of NO_x by C_3H_6 and NH_3. *Sci. Total Environ.* **2021**, *784*, 147394. [CrossRef] [PubMed]
98. Xu, Y.; Wu, X.; Lin, Q.; Hu, J.; Ran, R.; Weng, D. SO_2 promoted V_2O_5-MoO_3/TiO_2 catalyst for NH_3-SCR of NO_x at low temperatures. *Appl. Catal. A* **2019**, *570*, 42–50. [CrossRef]
99. Chen, L.; Shen, Y.; Wang, Q.; Wang, X.; Wang, Y.; Li, B.L.; Li, S.J.; Zhang, S.H.; Li, W. Phosphate on ceria with controlled active sites distribution for wide temperature NH_3-SCR. *J. Hazard. Mater.* **2022**, *427*, 128148. [CrossRef]
100. Xiang, G.; Ye, J.; Yi, Z.; Luo, Z.; Cen, K. The activity and characterization of CeO_2-TiO_2 catalysts prepared by the sol-gel method for selective catalytic reduction of NO with NH_3. *J. Hazard. Mater.* **2010**, *174*, 734–739.
101. Jiang, B.; Zhao, S.; Wang, Y.; Wenren, Y.; Zhu, Z.; Harding, J.; Zhang, X.L.; Tu, X.; Zhang, X.M. Plasma-enhanced low temperature NH_3-SCR of NO_x over a Cu-Mn/SAPO-34 catalyst under oxygen-rich conditions. *Appl. Catal. B* **2021**, *286*, 119886. [CrossRef]
102. Zhang, X.J.; Zhang, T.J.; Song, Z.X.; Liu, W.; Xing, Y. Effect of sulfate species on the performance of Ce-Fe-O catalysts in the selective catalytic reduction of NO by NH_3. *J. Fuel Chem. Technol.* **2021**, *49*, 844–852. [CrossRef]
103. Qi, G.; Li, W. NO oxidation to NO_2 over manganese-cerium mixed oxides. *Catal. Today* **2015**, *258*, 205–213. [CrossRef]
104. Qi, G.; Yang, R.T. Performance and kinetics study for low-temperature SCR of NO with NH_3 over MnO_x–CeO_2 catalyst. *J. Catal.* **2003**, *217*, 434–441. [CrossRef]
105. Gao, G.; Shi, J.W.; Liu, C.; Gao, C.; Fan, Z.Y.; Niu, C.M. Mn/CeO_2 catalysts for SCR of NO_x with NH_3: Comparative study on the effect of supports on low-temperature catalytic activity. *Appl. Surf. Sci.* **2017**, *411*, 338–346. [CrossRef]
106. Chen, J.; Fu, P.; Lv, D.F.; Chen, Y.; Fan, M.L.; Wu, J.L.; Meshram, A.; Mu, B.; Li, X.; Xia, Q.B. Unusual positive effect of SO_2 on Mn-Ce mixed-oxide catalyst for the SCR reaction of NO_x with NH_3. *Chem. Eng. J.* **2021**, *407*, 127071. [CrossRef]
107. Xiao, X.X.; Wang, J.T.; Jia, X.F.; Ma, C.; Qiao, W.M.; Ling, L.C. Low-Temperature Selective Catalytic Reduction of NO_x with NH_3 over Mn–Ce Composites Synthesized by Polymer-Assisted Deposition. *ACS Omega.* **2021**, *6*, 12801–12812. [CrossRef] [PubMed]
108. Lin, F.; Wang, Q.L.; Zhang, J.C.; Jin, J.; Lu, S.Y.; Yan, J.H. Mechanism and Kinetics Study on Low-Temperature NH_3-SCR Over Manganese–Cerium Composite Oxide Catalysts. *Ind. Eng. Chem. Res.* **2019**, *58*, 22763–22770. [CrossRef]
109. Wang, D.; Peng, Y.; Yang, Q.; Hu, F.; Li, J.; Crittenden, J. NH_3-SCR performance of WO_3 blanketed CeO_2 with different morphology: Balance of surface reducibility and acidity. *Catal. Today* **2019**, *332*, 42–48. [CrossRef]

110. Tan, H.; Ma, S.; Zhao, X.; Li, Y.; Zhao, C.; Zhu, Y. Excellent low-temperature NH_3 -SCR of NO activity and resistance to H_2O and SO_2 over WaCex (a = 0.06, 0.12, 0.18, 0.24) catalysts: Key role of acidity derived from tungsten addition. *Appl. Catal. A* **2021**, *627*, 118374. [CrossRef]
111. Yao, X.; Chen, L.; Cao, J.; Yang, F.; Tan, W.; Dong, L. Morphology and Crystal-Plane Effects of CeO_2 on TiO_2/CeO_2 Catalysts During NH_3-SCR Reaction. *Ind. Eng. Chem. Res.* **2018**, *57*, 12407–12419. [CrossRef]
112. Liu, J.; Li, X.Y.; Zhao, Q.D.; Ke, J.; Xiao, H.N.; Lv, X.J.; Liu, S.M.; Tadé, M.; Wang, S.B. Mechanistic investigation of the enhanced NH_3-SCR on cobalt-decorated Ce-Ti mixed oxide: In situ FTIR analysis for structure-activity correlation. *Appl. Catal. B* **2017**, *200*, 297–308. [CrossRef]
113. Andana, T.; Piumetti, M.; Bensaid, S.; Veyre, L.; Thieuleux, C.; Russo, N.; Fino, D.; Quadrelli, E.A.; Pirone, R. CuO nanoparticles supported by ceria for NO_x-assisted soot oxidation: Insight into catalytic activity and sintering. *Appl. Catal. B* **2017**, *216*, 41–58. [CrossRef]
114. Lin, F.; Wu, X.; Weng, D. Effect of barium loading on CuO_x–CeO_2 catalysts: NO_x storage capacity, NO oxidation ability and soot oxidation activity. *Catal. Today* **2011**, *175*, 124–132. [CrossRef]
115. Piumetti, M.; Bensaid, S.; Andana, T.; Russo, N.; Pirone, R.; Fino, D. Cerium-copper oxides prepared by solution combustion synthesis for total oxidation reactions: From powder catalysts to structured reactors. *Appl. Catal. B* **2017**, *205*, 455–468. [CrossRef]
116. Papavasiliou, J.; Rawski, M.; Vakros, J.; Avgouropoulos, G. A novel post-synthesis modification of CuO-CeO_2 catalysts: Effect on their activity for selective CO oxidation. *ChemCatChem* **2018**, *10*, 2096–2106. [CrossRef]
117. Konsolakis, M. The role of copper–ceria interactions in catalysis science: Recent theoretical and experimental advances. *Appl. Catal. B.* **2016**, *198*, 49–66. [CrossRef]
118. Zhao, K.; Han, W.L.; Lu, G.X.; Lu, J.Y.; Tang, Z.C.; Zhen, X.P. Promotion of redox and stability features of doped Ce–W–Ti for NH_3-SCR reaction over a wide temperature range. *Appl. Surf. Sci.* **2016**, *379*, 316–322. [CrossRef]
119. Li, Y.Y.; Zhang, Z.P.; Zhao, X.Y.; Liu, Z.; Zhang, T.R.; Niu, X.Y.; Zhu, Y.J. Effects of Nb-modified $CeVO_4$ to form surface Ce-O-Nb bonds on improving low-temperature NH_3-SCR deNO_x activity and resistance to SO_2 & H_2O. *Fuel* **2023**, *331*, 125799.
120. Wu, T.; Guo, R.T.; Li, C.F.; You, Y.H.; Pan, W.G. Recent advances in core-shell structured catalysts for low-temperature NH_3-SCR of NO_x. *Chemosphere* **2023**, *333*, 138942. [CrossRef]
121. Yu, L.; Zhong, Q.; Zhang, S.; Zhao, W.; Zhang, R. A CuO-V_2O_5/TiO_2 Catalyst for the Selective Catalytic Reduction of NO with NH_3. *Combust. Sci. Technol.* **2015**, *187*, 925–936. [CrossRef]
122. Wang, P.; Guo, R. The promotion effect of copper doping on the potassium resistance of V/TiO_2 catalyst for selective catalytic reduction of NO with NH_3. *Chem. Pap.* **2017**, *71*, 2253–2259. [CrossRef]
123. Zheng, Y.; Guo, Y.Y.; Shan, W.P.; Lian, Z.H.; Zhu, T.Y. Revealing the Ca resistance enhancement mechanism for the NH_3-SCR reaction over VTi catalyst by CuO modification. *Appl. Catal. A Gen.* **2022**, *637*, 118606. [CrossRef]
124. Raja, S.; Alphin, M.S.; Sivachandiran, L.; Singh, P.; Damma, D.; Smirniotis, P.G. TiO_2 -carbon nanotubes composite supported MnO_x-CuO catalyst for low-temperature NH_3 -SCR of NO: Investigation of SO_2 and H_2O tolerance. *Fuel* **2022**, *307*, 121886. [CrossRef]
125. Wang, H.; Zhu, T.; Qiao, Y.J.; Dong, S.C.; Qu, Z.P. Investigation of the promotion effect of Mo doped CuO catalysts for the low-temperature performance of NH_3-SCR reaction. *Chin. Chem. Lett.* **2022**, *33*, 5223–5227. [CrossRef]
126. Yu, Y.K.; Miao, J.F.; Wang, J.X.; He, C.; Chen, J.S. Facile synthesis of $CuSO_4/TiO_2$ catalysts with superior activity and SO_2 tolerance for NH_3-SCR: Physicochemical properties and reaction mechanism. *Catal. Sci. Technol.* **2017**, *7*, 1590. [CrossRef]
127. Shi, M.M.; Ye, S.; Qu, H.X.; Guo, L.; Zhong, Q. Synergistic effect of Cu^{2+} doping and sulfation in Cu-Ce-S, tolerance to H_2O and SO_2 and decomposition behaviors of ammonia salts. *Mol. Catal.* **2018**, *459*, 135–140. [CrossRef]
128. Yu, Y.K.; Chen, C.W.; He, C.; Miao, J.F.; Chen, J.S. In situ growth synthesis of CuO@Cu-MOFs core-shell materials as novel low-temperature NH_3-SCR catalysts. *ChemCatChem* **2019**, *11*, 979–984. [CrossRef]
129. Jiang, J.; Zheng, R.Z.; Jia, Y.; Guo, L.N.; Huang, M.Y.; Hu, J.; Xia, Y.J. Investigation of SO_2 and H_2O poisoning over Cu-HPMo/TiO_2 catalyst for Low temperature SCR: An experimental and DFT study. *Mol. Catal.* **2020**, *493*, 111044. [CrossRef]
130. Feng, S.; Li, Z.M.; Shen, B.X.; Yuan, P.; Ma, J.; Wang, Z.Z.; Kong, W.W. An overview of the deactivation mechanism and modification methods of the SCR catalysts for denitration from marine engine exhaust. *J. Environ. Manag.* **2022**, *317*, 115457. [CrossRef]
131. Chen, M.M.; Jin, Q.J.; Tao, X.J.; Pan, Y.C.; Gu, S.S.; Shen, Y.S. Novel W-Zr-O_x/TiO_2 catalyst for selective catalytic reduction of NO by NH_3 at high temperature. *Catal. Today* **2020**, *358*, 254–262. [CrossRef]
132. Feng, S.; Li, Z.M.; Shen, B.X.; Yuan, P.; Wang, B.; Liu, L.J.; Wang, Z.Z.; Ma, J.; Kong, W.W. High activity of NH_3-SCR at high temperature over W-Zr/ZSM-5 in the exhaust gas of diesel engine. *Fuel* **2022**, *323*, 124337. [CrossRef]
133. Jin, Q.J.; Shen, Y.S.; Ma, L.; Pan, Y.C.; Zhu, S.M.; Zhang, J.; Zhou, W.; Wei, X.F.; Li, X.J. Novel TiO_2 catalyst carriers with high thermostability for selective catalytic reduction of NO by NH_3. *Catal. Today* **2019**, *327*, 279–287. [CrossRef] [PubMed]